PLANT SCIENCES

The heat response regulators HSFA1s promote *Arabidopsis* thermomorphogenesis via stabilizing PIF4 during the day

Wenrong Tan[1]†, Junhua Chen[1]†, Xiaolan Yue[1], Shuli Chai[1], Wei Liu[1], Chenglin Li[1], Feng Yang[2], Yongfeng Gao[1], Lucas Gutiérrez Rodríguez[1], Víctor Resco de Dios[1,3], Dawei Zhang[2]*, Yinan Yao[1]*

During summer, plants often experience increased light inputs and high temperatures, two major environmental factors with contrasting effects on thermomorphological traits. The integration of light and temperature signaling to control thermomorphogenesis in plants is critical for their acclimation in such conditions, but the underlying mechanisms remain largely unclear. We found that heat shock transcription factor 1d (HSFA1d) and its homologs are necessary for plant thermomorphogenesis during the day. In response to warm daytime temperature, HSFA1s markedly accumulate and move into the nucleus where they interact with phytochrome-interacting factor 4 (PIF4) and stabilize PIF4 by interfering with phytochrome B–PIF4 interaction. Moreover, we found that the HSFA1d nuclear localization under warm daytime temperature is mediated by constitutive photomorphogenic 1–repressed GSK3-like kinase BIN2. These results support a regulatory mechanism for thermomorphogenesis in the daytime mediated by the HSFA1s-PIF4 module and uncover HSFA1s as critical regulators integrating light and temperature signaling for a better acclimation of plants to the summer high temperature.

INTRODUCTION

Light and temperature are two major environmental factors that profoundly influence the growth, development, and geographic distribution of plants, as well as the productivity of crop species (*1*–*3*). Plants use dynamic fluctuations in light and temperature as major information cues to optimize their growth and development programs to adapt to the ever-changing environmental conditions. For example, the hypocotyl of post-germinated seedlings elongates rapidly in the soil, enabling seedlings to reach the soil surface and perceive sunlight (*4*). Upon soil protrusion, light inhibits hypocotyl elongation, while seedling growth is sped up by shading from their neighbors (*5*, *6*). Moreover, ambient warm temperature also promotes hypocotyl elongation to facilitate cooling of heat-labile meristematic and photosynthetically active tissues, a process called thermomorphogenesis (*7*). Warm temperature thus tends to antagonize light signals in the regulation of hypocotyl growth (*8*). Because plants often experience warm temperatures and light inputs during the daytime, especially in summer, plants must continuously sense and integrate these two conflicting signals to improve thermomorphogenic acclimation. However, how plants integrate warm temperature and light signals to fine-tune their growth to better respond and acclimate to daytime high temperatures is not well understood yet.

The basic-helix-loop-helix transcription factor phytochrome-interacting factor 4 (PIF4), a key component of light signaling transduction that mediates skotomorphogenesis by promoting hypocotyl and petiole elongation, also acts as a central hub in the control of thermomorphogenesis (*9*, *10*). Both PIF4 transcript and its protein levels are induced by warm temperature, and then increased PIF4 activity promotes thermomorphogenic phenotypes including hyponasty, hypocotyl, and petiole elongation via activation of auxin synthesis enzymes (YUCCA8 and TAA1) and high-temperature responsive gene expression (*10*–*13*). Extensive evidence has shown that the strict regulation of PIF4 protein abundance and activity is essential for the integration of light and warm temperature signals into plant morphogenesis (*14*). More specifically, the photoreceptor phytochrome (phyB), also identified as the main thermosensor, controls the function of PIF4 at the sensor level in response to both fluctuating light and ambient temperatures in *Arabidopsis* (*15*–*17*).

PhyB senses changes in light conditions through two photo-interconvertible forms: a red light–absorbing inactive Pr and a far-red light–absorbing active Pfr (*17*, *18*). Under the dark or shade (i.e., with a low red/far-red light ratio) conditions, phyB is in the inactive Pr form and located in the cytosol; upon light irradiation, phyB is converted to the Pfr form and translocate into the nucleus, where phyB Pfr interacts with PIF4 to promote PIF4 degradation and inhibit its transcription activity, thereby initiating photomorphogenesis and suppressing hypocotyl growth (*19*–*21*). Conversely, warm temperatures facilitate the conversion of phyB from Pfr to the inactive Pr form, a process termed thermal reversion, which derepresses PIF4 and increases thermoresponsive genes expression to promote thermomorphogenic hypocotyl growth at high ambient temperatures (*15*, *16*, *22*). In addition, a recent study has shown that photo-activated phyB undergoes phase separation to assemble liquid-like droplets. Light induces allosteric changes of phyB and then alters its condensate assemblage, while temperature modulates the phase behavior of phyB droplets. These distinct regulatory patterns by light and temperature enable phyB to discriminate between

[1]School of Life Science and Engineering, Southwest University of Science and Technology, Mianyang, China. [2]Ministry of Education Key Laboratory for Bio-Resource and Eco-Environment, College of Life Sciences, Sichuan University, Chengdu, China. [3]Department of Crop and Forest Sciences & Agrotecnio Center, Universitat de Lleida, Leida, Spain.
*Corresponding author. Email: zhdawei@scu.edu.cn (D.Z.); yinanyao@swust.edu.cn (Y.Y.)
†These authors contributed equally to this work.

the two signals, selectively incorporating its interacting transcription factors into droplets (*23*).

In addition to the degradation and inactivation by phyB signaling, PIF4 is also controlled by the circadian clock at the transcriptional level (*24*). ELF3, a component of the clock oscillator, interacts with ELF4 and LUX to form a protein complex, called the evening complex, which directly binds to the promoter of PIF4 to inhibit gene expression during early night (*25*–*27*). Under warm conditions, the elevated temperatures promote the phase separation of the ELF3 PrD domain to form discrete condensates, an inactive form of ELF3, thereby releasing the inhibitory effect of ELF3 on PIF4 that triggers the thermomorphogenic responses (*28*). Collectively, these studies demonstrated that light, warm temperature, and circadian clock mainly converge on the regulation of PIF4 to control thermomorphogenesis.

Reality, however, is a bit more complex, because the thermo-enhanced hypocotyl elongation occurs at different contrasting time periods in short-day (SD) and long-day (LD) photoperiods (*29*). Under SD conditions, the warm temperature–induced hypocotyl elongation occurs mostly during the nighttime and this process is mainly mediated by ELF3 (*25*, *26*, *30*). By contrast, in LDs, the warm temperature–induced hypocotyl elongation mainly takes place during the day (*29*, *31*, *32*). The PHYB signaling pathway has been reported to mediate the daytime thermosensing in LDs or continuous light by regulating the activity and stability of PIF4 (*33*). Both PIF4 transcripts and proteins are mainly accumulated during the daytime in LDs or continuous light, which is consistent with the peak of elongation growth in the daytime (*24*, *29*, *32*). Warm temperature further accelerates the accumulation of PIF4 in the day (*10*, *32*, *33*). Because photoactivated phyB often promotes PIF4 degradation and inactivation, the warm temperature tends to compete with phyB signaling in the day. As a previous study has shown, the thermal reversion of phyB Pfr can offset a part of its photoactivation (*15*). Hemera (HMR) and Regulator of chloroplast biogenesis (RCB) were recently reported to jointly stabilize PIF4 in the daytime (*33*, *34*). However, plants often experience conditions of high temperatures combined with enhanced light inputs in the summer, when a substantial portion of photo-activated phyB is still present that enables plants to perform a series of light responses, such as photosynthesis. Therefore, to acclimate the warm conditions in summer, plants are required to separate the warm temperature and light signals to coordinate and adjust PIF4 protein under the daytime warm temperatures.

Heat shock transcription factors (HSFs) are highly conserved central regulators of heat stress (HS) response in animals, yeasts, and plants. They can control a large number of HS-responsive genes encoding heat shock proteins (HSPs) and other stress regulators through binding to the conserved heat shock cis-elements (nGAAnnTTCn) (*35*–*37*). The *Arabidopsis* genome has 21 HSF homologs that can be grouped into three classes (HSFA, HSFB, and HSFC), which are further divided into 14 groups including A1 to A9, B1 to B4, and C1 (*37*). Among them, the HSFA1 group, with four members (HSFA1a, 1b, 1d, and 1e), is considered as the master regulators indispensable for the activation of transcriptional networks in HS responses (*37*, *38*). More than 65% of heat-induced genes, including key transcription factors and HSPs essential for HS tolerance (such as *HSFA2*, *DREB2A*, *Hsp70*, and *Hsp90*), are compromised in the *hsfa1a/b/d/e* quadruple KO mutant (*QK*) (*39*, *40*). Studies on *hsfa1a/b/d/e* quadruple mutant and four triple knockout mutants have shown that HSFA1a, HSFA1b, and HSFA1d function redundantly to trigger heat shock response and confer thermotolerance, whereas HSFA1e seems to be less important for heat response (*39*). Similar phenotypes of *hsfa1a/b/d* triple mutant and *hsfa1a/b/d/e* quadruple mutant in thermotolerance support the hypothesis that HSFA1a, HSFA1b, and HSFA1d are the master regulators of HS response in *Arabidopsis* (*39*). Furthermore, HSFA1s confer a broad range of adverse environmental tolerances, including drought, salt, osmotic, and oxidative conditions (*41*–*43*). Recently, HSFA1 was shown to interact with the salicylic acid receptor NPR1, inducing HS-responsive genes including *Hsps* and *HSFA2*, thereby promoting cold acclimation (*44*). Several recent studies have revealed some of the potential roles of HSFA1 in the regulation of plant growth under adverse conditions. HSFA1d promotes hypocotyl elongation under chilling by activation of ribosomal protein gene expression, which maintains protein translation for growth (*45*). BIN2 and BES1, two central components of the Brassinosteriod (BR) signaling pathway, which is considered as a growth-related phytohormone pathway, were shown to interact with HSFA1 and affect its cellular localization and activity to regulate HS response (*46*, *47*). To summarize, the available evidence indicates that HSFA1 regulators not only regulate a broad range of responses to adverse conditions, but also participate in the regulation of plant growth. However, how HSFA1 regulators coordinate with environmental cues and the growth process to acclimate to fluctuating temperatures remains to be clarified.

Here, we provide direct evidence that heat response regulators HSFA1s interact with PIF4 and stabilize PIF4 through interfering with the interaction between PIF4 and photoactivated phyB under warm daytime temperatures, thereby promoting thermomorphogenesis during the day. Our results demonstrate that the protein accumulation and nuclear localization of HSFA1s are induced by warm temperatures while this induction is dependent on light. Furthermore, we found that E3 ligase constitutive photomorphogenic 1 (COP1), a regulator of photomorphogenesis and thermomorphogenesis, mediates the translocation of HSFA1d to nuclear through inhibiting BIN2-directed phosphorylation of HSFA1d. Collectively, our study uncovers a critical role of HSFA1s in regulation of daytime thermomorphogenesis, promoting PIF4 accumulation in the warm daytime conditions. HSFA1 thus represents an integration node for light and warm temperature signaling, facilitating improved responses and acclimation of plants to daytime warm conditions.

RESULTS

PIF4 interacts with HSFA1d

Temperate plants grown under natural summer conditions with long photoperiods and high temperatures during the daytime showed notable thermomorphogenesis (*48*). However, how plants modulate PIF4 activity and its stabilization in such conditions is not fully understood. To identify the regulator of PIF4 under the warm daytime temperatures, we grew wild-type *Arabidopsis* (Col-0) in continuous light (120 μmol m^{-2} s^{-1} white light) at 28°C, and then collected the whole seedlings to generate a cDNA yeast library and performed a yeast two-hybrid screening using BD-PIF4 as a bait. Among the putative PIF4-interacting proteins, HSFA1d, a key regulator of heat response, displayed a strong interaction with PIF4. We also performed an independent yeast two-

hybrid experiment to verify the interaction between PIF4 and HSFA1d (Fig. 1A). Yeast two-hybrid assays with truncated PIF4 further revealed that the N terminus including the APB motif (amino acids 1 to 135; Fig. 1B) of PIF4 mediates its interaction with HSFA1d (Fig. 1, B and C). Subsequently, we examined the HSFA1d functional domains required for PIF4-HSFA1d interaction by using in vitro pull-down assays. The HSFA1d N terminus contains a DNA binding domain (DBD, HSFA1d-S1, amino acids 1 to 144) and the S2 domain including an oligomerization domain (HR-A/B) and a nuclear localization signal (NLS) (HSFA1d-S2, amino acids 145 to 260); the HSFA1d C terminus consists of the S3 domain (HSFA1d-S3, amino acids 261 to 418) and the S4 domain including the transactivation motif (AHA) plus a nuclear export signal NES motif (HSFA1d-S4, amino acids 419 to 485) (fig. S1A). MBP-tagged HSFA1d, HSFA1d-S1, HSFA1d-S2, HSFA1d-S3, and HSFA1d-S4, and HIS-tagged PIF4 were all expressed and purified from *Escherichia coli*. HIS-PIF4 could pull down MBP-HSFA1d, MBP-HSFA1d-S1, and MBP-HSFA1d-S2, but none of MBP, MBP-HSFA1d-S3, and MBP-HSFA1d-S4. This implied that PIF4 could interact with HSFA1d and the N terminus of HSFA1d directly in vitro (Fig. 1D and fig. S1B). To determine which region of the HSFA1d N terminus confers its interaction with PIF4, we examined the interaction between PIF4 and two truncation fragments of the HSFA1d N terminus: MBP-HSFA1dΔS1 and MBP-HSFA1dΔS2 (fig. S1C). HIS-PIF4 could only pull down MBP-HSFA1dΔS2, but not MBP-HSFA1dΔS1 and MBP, suggesting that the S1 domain of HSFA1d is essential for its interaction with PIF4 (fig. S1D).

Next, we determined whether PIF4 interacts with HSFA1d in plants by performing firefly luciferase complementation imaging (LCI) assays and bimolecular fluorescence complementation (BiFC) assays in *Nicotiana benthamiana* leaves. As shown in Fig. 1E, we only detected a weak luciferase signal in *N. benthamiana* leaves coexpressing PIF4-NLuc and HSFA1d-CLuc at 21°C, whereas a strong luminescence could be detected, when shifting the *N. benthamiana* to 28° and continuous light conditions for 24 hours

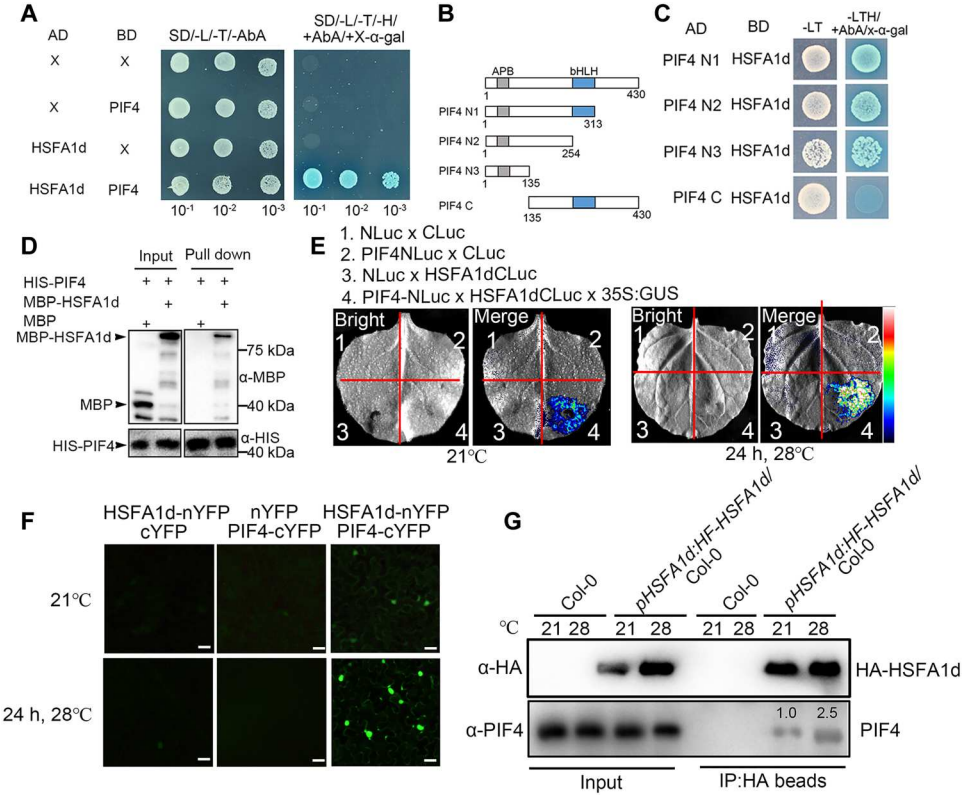

Fig. 1. HSFA1d directly interacts with PIF4. (**A**) Yeast two-hybrid assays to confirm the interaction between HSFA1d and PIF4. The interaction clones were selected on the synthetic dropout medium (SD/−Leu/−Trp/−His/+Aba/+X-α-gal) plus 5 mM 3-AT. (**B**) Schematic diagram of various fragments of PIF4 used in (C). The numbers indicate the positions of amino acids. (**C**) Deletions of the PIF4 protein were used to map the interacting domain via yeast two-hybrid assays. Yeast clones were grown on the synthetic dropout medium plus 5 mM 3-AT. (**D**) In vitro pull-down assays to detect the interaction of HSFA1d with PIF4. Recombinant MBP or MBP-HSFA1d were incubated with His-PIF4 bound to the Ni-NTA agarose beads. The MBP-HSFA1d proteins pulled down with HIS-tagged PIF4 were detected using anti-MBP antibody. (**E**) Luciferase complementation imaging (LCI) assays showing in vivo protein interactions. Empty vectors were used as negative controls. *35S:GUS* was used as a temperature-insensitive control. The vectors combined as indicated in top panel were cotransformed into *Nicotiana benthamiana* leaves and those plants were then grown at either 21° or 28°C for 24 hours before imaging. (**F**) BiFC assays showed that HSFA1d interacts with PIF4 in the epidermal cells of *N. benthamiana* leaves under either 21° or 28°C for 24 hours. Reconstitution of YFP was shown. Scale bars, 20 μm. (**G**) The interaction between HSFA1d and PIF4 in plants was detected by CoIP assays. Seedlings of wild type (Col-0) and Col-0 plants expressing *pHSFA1d:HF-HSFA1d* were grown at 21° or 28°C under LDs for 5 days. Proteins extracted from the seedlings were incubated with HA-Trap agarose beads, the HA-FLAG (HF)–tagged HSFA1d was examined by anti-HA antibody, and the coimmunoprecipitated PIF4 proteins were detected by anti-PIF4 antibody.

(Fig. 1E). The expression of the fusion proteins and luciferase activity were examined (fig. S1, E to G). The results showed that PIF4-Nluc protein increased about 1.5-fold and HSFA1d-Cluc protein increased about 1.7-fold under warm temperatures, while the luciferase activity increased about 60-fold in *N. benthamiana* grown at 28°C compared to that in 21°C, suggesting that warm temperature greatly enhances the interaction between PIF4 and HSFA1d in plant. The BiFC assays further revealed that PIF4 interacted with HSFA1d mainly in the nucleus and that this interaction was substantially enhanced by warm temperature (Fig. 1F).

Complementarily, a coimmunoprecipitation assay was performed in Col-0 and *pHSFA1d: HF-HSFA1d*/Col-0 transgenic plant in which Hemagglutinin (HA)–FLAG-tagged HSFA1d was driven by its own promoter. The results showed that much more PIF4 proteins were coprecipitated with HF-HSFA1d at warm temperature than under normal conditions (Fig. 1G). These results suggested that PIF4 interacts with HSFA1d in vitro and in vivo, and that warm temperature strongly promotes the formation of PIF4-HSFA1d protein complex.

In addition, to confirm whether the PIF4-HSFA1d interaction were stable or not, we further performed a chromatin immunoprecipitation (ChIP) quantitative polymerase chain reaction (PCR) assay using *pHSFA1d: HF-HSFA1d*/Col-0 grown at either 21° or 28°C under LDs. The results showed that the binding of HSFA1d to the G box motif of the *YUC8* promoter that PIF4 binds to was hardly detected under 21°C, whereas the association between HSFA1d and the promoter regions of *YUC8* was greatly enhanced by warm temperature (fig. S1H). These results demonstrated that HSFA1d can form a stable complex with PIF4 in vivo under warm temperatures.

HSFA1d functions redundantly with its homologs HSFA1a and HSFA1b to promote thermomorphogenesis during the day

Given the central role of PIF4 in plant thermomorphogenesis, e.g., mediating hypocotyl growth in response to warm temperature, it is possible that HSFA1d acts as a potential regulator in thermomorphogenesis. HSFA1d-deficient mutants *hsfa1d-1* and *hsfa1d-2* showed hypocotyl elongation similar to wild-type plants (Col-0) at 28°C under LDs (16 hours light/8 hours dark, 120 μmol m^{-2} s^{-1} white light), whereas the hypocotyls of *HSFA1d*-overexpressing transgenic lines, *HSFA1d OE#1* and *HSFA1d OE#2*, were much longer elongated under the effect of warm temperatures in LDs, indicating that HSFA1d promotes warm growth response, and may function redundantly with its homologs (Fig. 2, A and C).

To investigate the redundant roles of HSFA1s including HSFA1a, HSFA1b, HSFA1d, and HSFA1e in thermomorphogenesis, we further determined the hypocotyl elongation of four triple mutants of HSFA1s including *hsfa1b/1d/1e* (*aTK*), *hsfa1a/1d/1e* (*bTK*), *hsfa1a/1b/1e* (*dTK*), and *hsfa1a/1b/1d* (*eTK*) at either 21° or 28°C under LDs. We observed thermo-insensitive phenotypes in *eTK*, while detecting no difference in hypocotyl growth between each of the other triple mutants (*aTK, bTK*, and *dTK*) and wild type (Col-0 and Ws) at 28°C under LDs, suggesting that HSFA1a and HSFA1b have overlapping functions with HSFA1d in thermomorphogenic hypocotyl growth (Fig. 2, B and D, and fig. S5, A and B). We also detected the interaction of PIF4 with other HSFA1 factors and found that PIF4 could interact with HSFA1a and HSFA1b, but not HSFA1e in yeast and plants, and these interactions are much weaker than the interaction between PIF4 with HSFA1d at 28°C; therefore, we mainly investigated the roles of HSFA1d in modulating PIF4 function thereafter (fig. S2, A to F). Under the control of their own native promoter, introduction of *HF-HSFA1a*, *HF-HSFA1b*, and *HF-HSFA1d* into *eTK* respectively resulted in the rescue of thermo-insensitive phenotypes of *eTK*, which further confirmed the redundant roles of HSFA1a, HSFA1b, and HSFA1d in thermomorphogenesis (fig. S2, G and H). We then measured the hypocotyl growth kinetics of Col-0, *HSFA1d OE*, and *eTK* seedlings at 28°C, the warm temperature–induced hypocotyl elongation mainly occurred during the daytime in Col-0, and this elongation was notably enhanced in *HSFA1d OE* and abolished in *eTK* (Fig. 2E). Altogether, these results provide genetic evidence that HSFA1d functions redundantly with HSFA1a and HSFA1b to promote the daytime thermomorphogenesis under LD conditions.

To further examine the thermal response of hypocotyl growth under SD and continuous dark conditions, Col-0 and *HSFA1d OE* lines and *eTK* mutants were grown at either 21° or 28°C under SDs (8 hours light/16 hours dark) or under constant dark conditions. As shown in fig. S3 (A to C), the warm temperature–induced hypocotyl elongation in wild type occurred mostly during the nighttime under SDs and *eTK* mutant showed a thermo-morphogenetic growth pattern similar to Col-0 (i.e., with a hypocotyl elongation during the night at 28°C), whereas the hypocotyl of HSFA1d-overexpressing plants displayed continuous thermomorphogenic elongation in both day and night under SDs, indicating that HSFA1s do not affect the thermomorphogenic growth at night, but promote hypocotyl elongation in the warm daytime under SDs. However, under constant darkness, the hypocotyl lengths of *HSFA1d OE* lines and *eTK* mutant were identical to the wild type and without showing any additional elongation at 28°C (fig. S3, D and E). These results further proved that HSFA1s promote thermomorphogenic growth during the daytime under both LD and SD conditions, but they do not affect the warm temperature response of hypocotyl growth at night.

To test whether HSFA1 factors regulate warm activation of PIF4 activity at a posttranscriptional level, we examined the transcriptional levels of *PIF4* and its well-characterized target gene *YUCCA8* (*YUC8*) at multiple time points of a diurnal light/dark 24-hour cycle (LDs, 16 hours light/8 hours dark) at either 21° or 28°C in Col-0, *HSFA1d OE#1*, and *eTK* seedlings. Consistent with the previous report (*32*), the expression of *PIF4* and *YUC8* genes was induced by warm temperature during the day under LDs in Col-0 seedlings (Fig. 2, F and G). Thermal induction of *YUC8* was enhanced in HSFA1d overexpression plants, but extinguished in *eTK* (Fig. 2, F and G). However, the warm temperature–dependent induction of *PIF4* was unaffected by HSFA1 factors, indicating that HSFA1s regulate PIF4 activity at the posttranscriptional level.

PIF4 pathway is required for HSFA1-promoted hypocotyl growth during thermomorphogenesis

PIF4 mediates hypocotyl thermomorphogenesis through controlling a large number of thermoresponsive genes. To determine whether HSFA1 factors are involved in this process, we compared the transcriptome of warm-treated *eTK* mutant with PIF4 direct targets, which were available from a public database (*49*). We identified 1178 genes targeted by PIF4 that were regulated by HSFA1s at

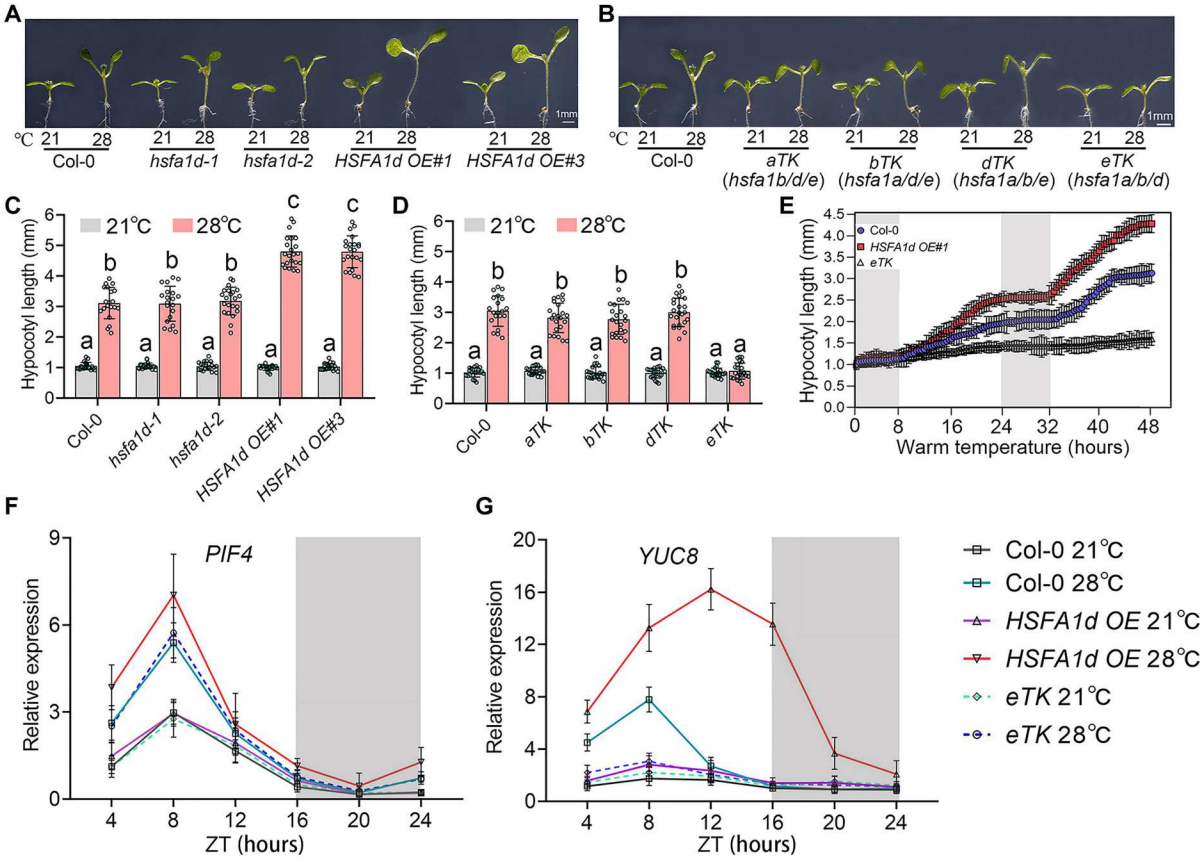

Fig. 2. HSFA1s promote thermomorphogenic hypocotyl growth and warm-temperature induction of PIF4 target in the daytime. (**A** and **B**) Representative images of 5-day-old Col-0, *HSFA1d OE*, and *hsfa1d* seedlings (A) and Col-0, *hsfa1b/1d/1e* (*aTK*), *hsfa1a/1d/1e* (*bTK*), *hsfa1a/1b/1e* (*dTK*), and *hsfa1a/1b/1d* (*eTK*) seedlings (B) grown at either 21° or 28°C under long days (LDs, 16 hours light/8 hours dark, 120 mmol m^{-2} s^{-1}). (**C** and **D**) Hypocotyl length of seedlings in (A) and (B). Error bars represent S.D. ($n = 20$). Different letters indicate statistically significant differences between samples (two-way ANOVA followed by a Tukey's HSD test, $P < 0.05$). (**E**) Kinetics of hypocotyl thermomorphogenesis under LDs. Wild-type, *HSFA1d OE*, and *eTK* seedlings were grown on 1/2 MS agar plates at 21°C under LD for 3 days and further grown at 28°C for another 2 days. Infrared images of seedlings were analyzed every 30 min. Error bars represent ±S.D. (**F** and **G**) Analysis diurnal levels of the transcripts of *PIF4* (F) and *YUC8* (G) genes in wild-type, *HSFA1d OE*, and *eTK* seedlings. These seedlings were grown in LDs at either 21° or 28°C for 5 days. Samples were collected every 4 hours during a cycle of 24 hours. *ACTIN2* was used as an internal control and presented as values relative to that of wild type at 21°C. Error bars represent the S.D. from three biological replicates. ZT is zeitgeber time.

28°C. Gene ontology (GO) analysis of these 1178 genes revealed that the genes involved in response to hypoxia, response to light intensity, response to auxin, response to red or far-red light, and regulation of hormone levels that are targeted by PIF4 were enriched in HSFA1-affected genes at 28°C (Fig. 3, A and B). We further confirmed that several well-characterized thermo-induced genes (i.e., *SAUR20*, *XTR6*, *ST2A*, *CDF5*, and *5PTASE11*), were highly up-regulated in wild types (Col-0 and Ws), but not up-regulated in *eTK* and *pif4-101* in warm temperature (Fig. 3, C to G, and fig. S5, D to I). These results showed that HSFA1 factors are associated with PIF4 in controlling a set of thermoresponsive gene expression.

To further investigate the genetic link between HSFA1s and PIF4, we crossed the *eTK* triple mutant with the *pif4-101* mutant. We detected no additive effects in the *eTK/pif4-101* mutants, which exhibited a similar thermo-insensitive phenotype to *pif4101* or *eTK* mutant, indicating that HSFA1 factors and PIF4 may act in concert (Fig. 3, H and I). We also crossed *35S:HSFA1d-GFP* (*HSFA1d OE*) with the *pif4-101* mutant. As shown above, *HSFA1d OE* plants displayed an enhanced thermoresponsive hypocotyl elongation as compared with Col-0, whereas *HSFA1d OE/pif4-101* seedlings exhibited a reduced hypocotyl growth at 28°C, similar to what observed in the *pif4–101* mutant (Fig. 3, H and J), indicating that HSFA1-promoted thermoresponsive hypocotyl growth is dependent on PIF4.

HSFA1 factors mediate the thermoresponsive PIF4 accumulation during the daytime

We next determined how does HSFA1s regulate PIF4 functions. Many interactors of PIF4, such as ELF3, CRY1, BES1/BZR1, TCP5/TCP13/TCP7, and FCA, have been previously shown to mainly affect the DNA-binding ability and transcriptional activity of PIF4 (*50*–*56*). Thus, we first investigated whether HSFA1d regulates the activity of PIF4 to its target genes. Electrophoretic mobility shift assays using PIF4 and HSFA1d proteins expressed in vitro were performed to detect the influence of HSFA1d on PIF4 DNA-binding ability. PIF4 bound to the promoter region of *YUC8* as reported before (*53*), and HSFA1d could not affect the DNA binding of PIF4 (fig. S4A). The transient transcription assay using *luciferase*

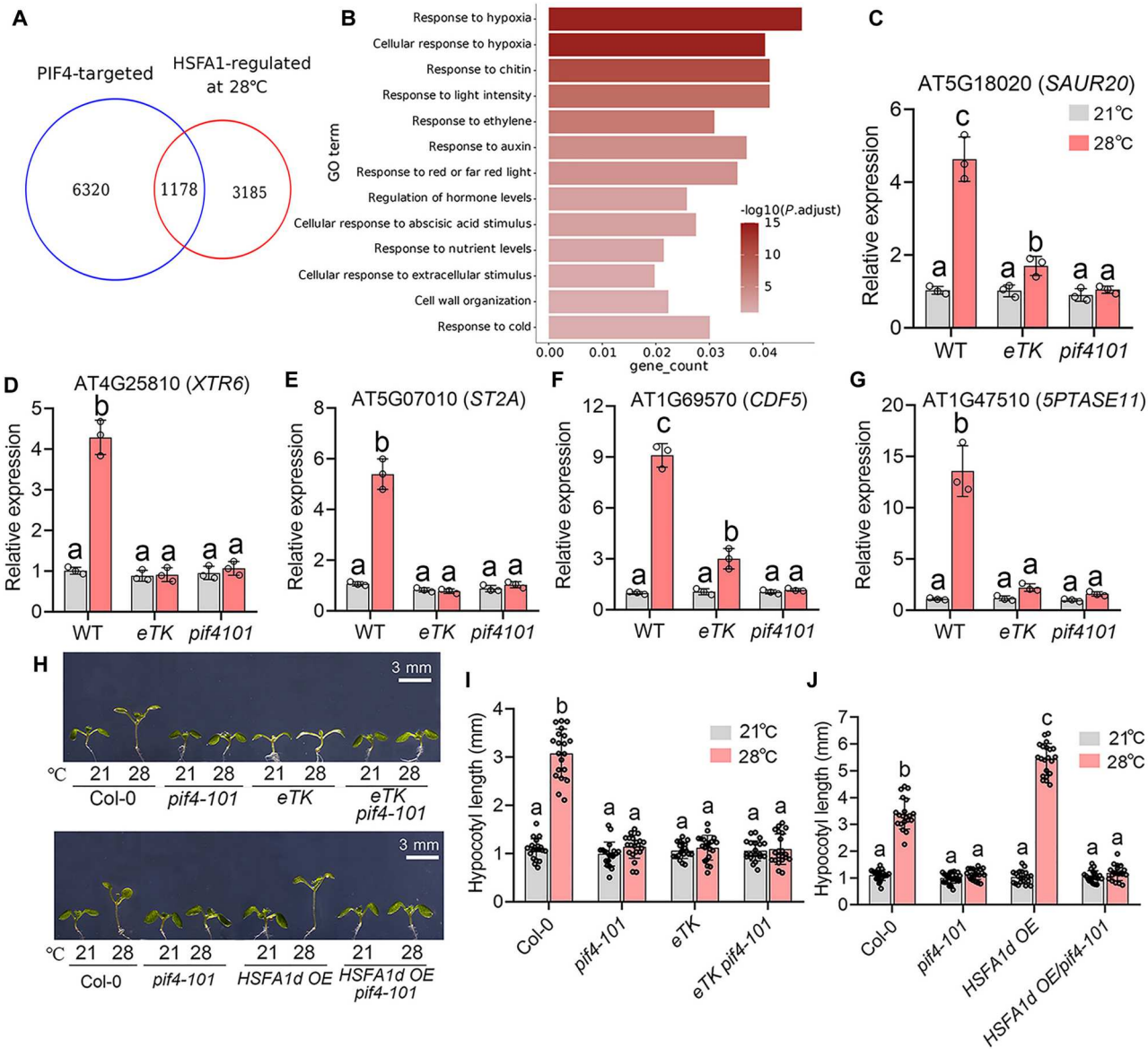

Fig. 3. HSFA1s are involved in PIF4-mediated hypocotyl thermomorphogenesis. (**A**) Venn diagram showing the overlapping genes coregulated by HSFA1s and PIF4. PIF4 targets represent the previously identified PIF4 direct target genes by ChIP-Seq. HSFA1-regulated genes at 28°C represent the differential genes between Col-0 and *eTK* at 28°C. (**B**) GO analysis of overlapping genes in (A). (**C** to **G**) RT-qPCR analyses for validation of gene expression patterns obtained from RNA-seq. *ACTIN2* was used as an internal control and presented as values relative to that of wild type at 21°C. Error bars represent the S.D. from three biological replicates. Different letters indicate statistically significant differences between samples (two-way ANOVA followed by a Tukey's HSD test with $P < 0.05$). (**H**) Representative images of 5-day-old Col-0, *eTK*, *pif4101*, *eTK/pif4101*, *HSFA1d OE*, and *HSFA1d OE/pif4101* seedlings grown at either 21° or 28°C under long days (LDs, 16 hours light/8 hours dark, 120 μmol m^{-2} s^{-1}). (**I** and **J**) Hypocotyl length of seedlings in (H). Error bars indicate S.D. ($n = 20$). Different letters indicate statistically significant differences between samples (two-way ANOVA with a Tukey's HSD test, $P < 0.05$).

(*LUC*) gene driven by the *YUC8* promoter (*pYUC8:LUC*) as a reporter again showed that HSFA1d did not regulate the transcriptional activity of PIF4 (fig. S4B). When we crossed *35S:PIF4-MYC* (*PIF4OX*) into the *eTK* background (*PIF4OX/eTK*), the daytime thermo-induced hypocotyl elongation of *PIF4OX* was abolished (Fig. 4, A and B). The protein level of PIF4-MYC was higher in *PIF4OX* plants grown at 28°C than in those grown at 21°C, while PIF4-MYC protein level in *PIF4OX/eTK* was insensitive to warm temperature and had no difference to *PIF4OX* at 21°C, indicating that HSFA1s facilitate thermo-induced PIF4 accumulation, but do not affect PIF4 stability at 21°C (Fig. 4C). Next, we assessed protein stability of PIF4 during the transition from 21 to 28°C. Our data showed that the PIF4 protein levels increased during the 21° to 28°C transition in Col-0 seedlings and that PIF4 proteins accumulated much more in *HSFA1d OE* seedlings at 28°C than that in Col-0. However, warm-induced PIF4 accumulation was totally abolished in *eTK* (Fig. 4, D and E). The thermo-induced PIF4 accumulation in *hsfa1d* single mutant and other HSFA1s triple mutants (*aTK*, *bTK*,

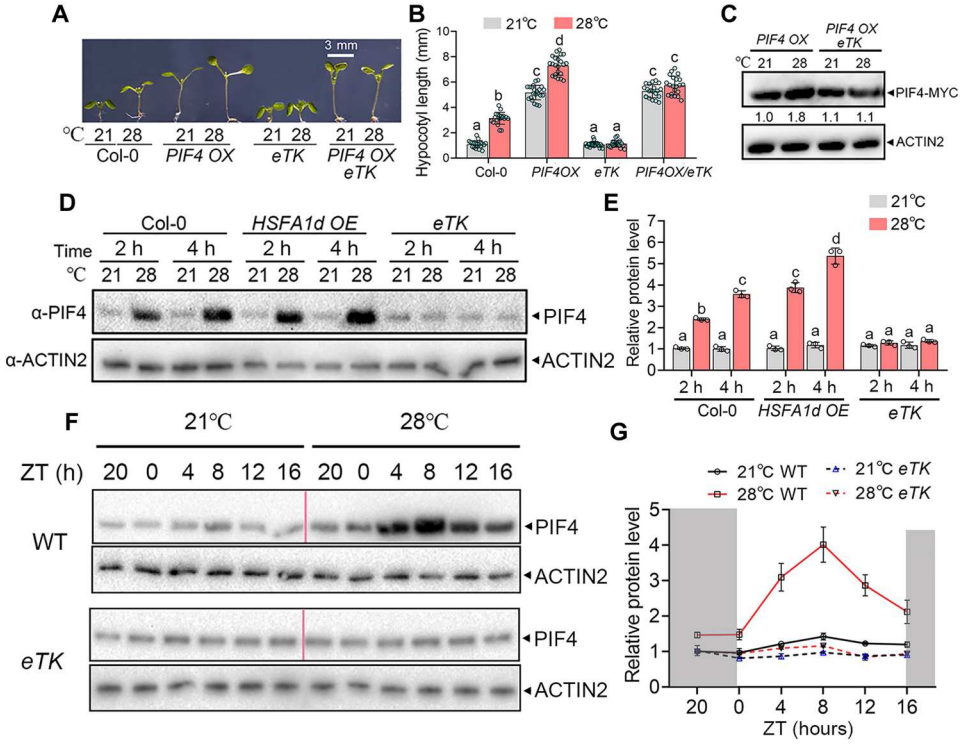

Fig. 4. HSFA1s promote the thermo-induced PIF4 accumulation. (**A** and **B**) Hypocotyl lengths of different genotype seedlings. Seedlings were grown at control 21° or 28°C under LDs for 5 days. (**C**) Immunoblot analysis showing the levels of PIF4-MYC in *PIF4OX* and *PIF4OX*/ *eTK* seedlings. Total proteins were extracted at ZT 8 hours from the seedlings grown in LDs at either 21° or 28°C for 5 days. ACTIN2 was used as a loading control. (**D**) Immunoblot analysis of PIF4 protein levels in Col-0, *HSFA1d OE*, and *eTK* seedlings during the transition from 21° to 28°C. The 5-day-old seedlings grown at 21°C under LDs, afterward transferring these plants to 28°C at ZT0 under LDs, and the samples were harvested after 2-hour and 4-hour treatment of 28°C. (**E**) Quantification of PIF4 proteins shown in (D). Relative protein levels of PIF4 are presented as values relative to ACTIN2 levels. (**F**) Diurnal levels of accumulation of PIF4 proteins in Col-0 and *eTK* seedlings. Seedlings were grown in LDs at either 21° or 28°C for 5 days. Then, the samples were collected every 4 hours during a cycle of 24 hours. (**G**) Quantification of PIF4 proteins in the Western blots shown in (F). The intensities of detected bands were quantified from three independent experiments using ImageJ. Protein levels were normalized relative to ACTIN2 and expressed relative to the levels at 21°C-grown Col-0 seedlings at ZT0. Error bars indicate S.D. ($n = 20$) in (B) and S.D. ($n = 3$) in (E) and (G). Different letters indicate significant differences (two-way ANOVA with a Tukey's HSD test, $P < 0.05$).

and *dTK*) was similar to that in wild-type plants at 28°C, indicating that HSFA1 factors redundantly promote thermoresponsive accumulation of PIF4 protein (fig. S6). Then, we determined the diurnal accumulation pattern of PIF4 protein in Ws and *eTK* seedlings at either 21° or 28°C under LDs. As shown in Fig. 4 (F and G), elevated temperatures markedly enhanced PIF4 protein levels in wild-type seedlings during the day, but this promotion was abolished in *eTK* seedlings, indicating that HSFA1 factors mediate the thermo-induced PIF4 accumulation during the daytime. However, under SDs conditions, warm temperature promotes PIF4 accumulation mainly during the night (ZT8-ZT24) in wild-type seedlings, and *eTK* mutant showed a similar pattern of PIF4 accumulation to wild type, while warm temperature–induced PIF4 accumulation occurred in both day and night in HSFA1d-overexpressing plants, which demonstrated that HSFA1 factors promote PIF4 protein accumulation in the warm daytime, but do not affect PIF4 protein accumulation during the nighttime under SD conditions (fig. S7, A and B).

To further estimate whether HSFA1s function on PIF4 stabilization, we detected the PIF4 proteins in Col-0, *HSFA1d OE*, and *eTK* mutant treated with/without cycloheximide (CHX) or CHX and MG132 at 28°C. As shown in fig. S7 (C and D), CHX application led to a rapid reduction of PIF4 protein abundance in Col-0, while the disappearing rate of PIF4 is much slower in *HSFA1d OE* seedlings and faster in *eTK* mutant than that in Col-0. At the same time, MG132 application effectively inhibited PIF4 degradation in Col-0 and *eTK* mutant, and the PIF4 protein abundance in Col-0 and *eTK* reached similar levels to those in HSFA1d OE seedling by 90 min of CHX and MG132 treatment (fig. S7, E and F). These data further demonstrated that HSFA1s stabilize PIF4 by preventing its degradation.

HSFA1d offsets phyB-mediated inhibition of PIF4 function

Another question is how do HSFA1s as transcription factors regulate the protein stability of PIF4 under daytime warm temperature. phyB, the main photoreceptor and also a thermosensor, was previously demonstrated to interact with PIF4 and induce its rapid turnover in response to light (*15*, *16*, *21*, *57*, *58*). As demonstrated above (Fig. 1C), the N terminus that includes the APB domain (the active phytochrome binding motif) of PIF4 mediates its interaction with HSFA1d; it is highly possible that HSFA1s, especially HSFA1d, regulate PIF4 function via the phyB pathway. We therefore determined whether HSFA1d inhibits the combination of phyB with PIF4. Firstly, we performed yeast three-hybrid assays to examine the

effects of HSFA1d on the interaction between phyB and PIF4. As PIF4 interacts selectively with the Pfr form of phyB, we used the chromophore phycocyanobilin (PCB) to facilitate phyB to form Pfr in yeast cells upon red (R) light irradiation. Consistent with previous reports (*57*, *59*, *60*), we observed that PIF4 interacts with phyB mainly in those yeast cells irradiated by R light, but not in those cells irradiated by far-red light (where phyB mainly existed as inactive Pr form). Coexpression of HSFA1d, AD-PIF4, and phyB-BD in yeast cells resulted in a markedly decreased interaction between phyB and PIF4, whereas HSFA1dΔS1, which lacks the domain of HSFA1d required for its interaction with PIF4, failed to inhibit phyB-PIF4 interaction, suggesting that HSFA1d and phyB competitively interact with PIF4 (Fig. 5A).

To confirm the inhibition of the interaction between phyB and PIF4 by HSFA1d in plants, we conducted LCI assays to detect the interaction between PIF4-nLuc and CLuc-phyB in the presence or absence of HSFA1d in *N. benthamiana* leaves. Our results show that coexpression of PIF4-nLuc and CLuc-phyB led to a strong luciferase activity in the absence of HSFA1d-GFP (green fluorescent protein), while coexpression of HSFA1d-GFP resulted in a substantial inhibition of the interaction between PIF4-nLuc and CLuc-phyB (Fig. 5, B and D). Nonetheless, coexpression of HSFA1dΔS1 did not affect the interaction between phyB and PIF4 in *N. benthamiana* (Fig. 5, C and E).

We also performed CoIP assays. We expressed HA-phyB in Col-0 or *pif4-101* protoplast cells and then performed anti-HA IP assays. Our data show that PIF4 was indeed coprecipitated with HA-phyB in the Col-0 protoplast irradiated with red light, but not in the Col-0 protoplast under far-red light treatment or in the *pif4-101* protoplast cells. However, when we coexpressed increasing amounts of HSFA1d-GFP, the amounts of PIF4 coprecipitated with HA-phyB markedly decreased, indicating that HSFA1d inhibits the formation of phyB-PIF4 complex in vivo (Fig. 5F). Together, these results point out that HSFA1d inhibits photoactive phyB interaction with PIF4.

To investigate the functional link between HSFA1d and phyB, we overexpressed the *HSFA1d* gene in the *35S:YHB* background, overexpressing a constitutively active phyB form harboring a $Y^{276}H$ substitution (YHB) (fig. S8, A and B). As shown in Fig. 5 (G and H), the thermomorphogenic responses are largely diminished in *35S:YHB* transgenic plants, whereas HSFA1d overexpression can partially rescue the thermo-insensitive hypocotyl growth of *35S:YHB* plants (Fig. 5, G and H). Notably, thermo-induced PIF4 levels in *HSFA1d OE/35S:YHB* plants were restored to that of wild type (Fig. 5I and fig. S8D). Consistently, the suppressive effect of active phyB of *35S:YHB* on the *YUC8* expression was largely compromised in *HSFA1d OE/35S:YHB* plants (fig. S8C). Collectively, these results illustrate that HSFA1d offsets phyB-mediated inhibition of PIF4 function.

Daytime warm temperature induces the accumulation and nuclear localization of HSFA1s

A central issue still remains to be thoroughly explained; i.e., how does HSFA1s integrate daytime warm temperature into the phyB-PIF4 pathway to regulate the themomorphogenic hypocotyl growth? To address this question, we first determined diurnal accumulation patterns of the HSFA1s factors in plants grown under LDs at either 21° or 28°C. Because of the representative role of HSFA1d in modulating PIF4 functions, we detected the accumulation patterns of HSFA1d proteins. Similar to PIF4 protein, HSFA1d proteins were detected reaching notable levels during the daytime and rapidly dropping after dusk (Fig. 6, A and B). Warm temperature markedly enhanced daytime accumulation of HSFA1d protein, although we detected warm-induced HSFA1d accumulation impaired at night, indicating that warm-temperature stabilization of HSFA1d may be dependent on light (Fig. 6, A and B). To test this hypothesis, we further assessed HSFA1d protein levels in seedlings grown under different light conditions. Our data show that warm temperature failed to induce HSFA1d accumulation in the dark-grown seedlings, whereas HSFA1d could accumulate rapidly at 28°C in the seedlings grown under different light regimes including white (W), red (R), but slightly under blue light (B), indicating that warm temperature induced HSFA1d accumulation in the light (Fig. 6, C to J).

To further explore whether high temperature modulates HSFA1d accumulation in the light via affecting its biosynthesis or stabilization, we first examined diurnal rhythms of *HSFA1d* transcripts at either 21° or 28°C under LDs. As shown in fig. S9A, consistent with the rhythmic patterns of its protein accumulation, *HSFA1d* gene was up-regulated in warm temperature–treated Col-0 seedlings during the daytime under LDs (fig. S9A). We then detected the levels of accumulation of HSFA1d-GFP proteins in *35S:HSFA1d-GFP* seedlings treated with CHX and MG132 in different light conditions. As shown in fig. S9B, CHX and MG132 application did not have any effect on HSFA1d in *HSFA1d-GFP* seedlings treated with 28°C in the dark. However, warm-induced HSFA1d accumulation in the white and red light was totally impaired by CHX and MG132 treatment. These data suggested that warm temperature modulates HSFA1d accumulation in the light via affecting its biosynthesis but not its stabilization.

The subcellular localization of HSFA1d was also affected by the warm temperature under the effect of light. Transient transformation assays in mesophyll protoplasts showed that HSFA1d is mainly localized in cytoplasm under the normal temperature, while warm temperature could induce HSFA1d translocation to nucleus under white light or red light. However, darkness could inhibit the nuclear localization of HSFA1d in response to warm temperature (Fig. 7, A and B, and fig. S9C). Consistently, at the root tips and hypocotyls of HSFA1d-GFP transgenic plants, HSFA1d mainly localizes in cytoplasm at 21°C, whereas warm temperature promotes HSFA1d nuclear localization in the light (Fig. 7C and fig. S9D). Then, HSFA1d proteins in the nucleus and cytoplasm fractions under different conditions were detected by cell fractionation followed by immunoblot. In seedlings grown under 21°C either in light or dark, or under 28°C in dark, HSFA1d was primarily localized in the cytoplasm. However, when grown under warm temperature in light, HSFA1d was detected mainly in the nuclear fraction (fig. S9E). We also investigated the effects of daytime warm temperature on the subcellular localization of HSFA1a and HSFA1b using transient transformation assays in tobacco leaves in the light. Consistent with the pattern of HSFA1d, both HSFA1a and HSFA1b translocated to nucleus at 28°C in the light (fig. S10, A to D). Altogether, these results strongly support that warm temperature induces HSFA1 factors′ nuclear localization in the light.

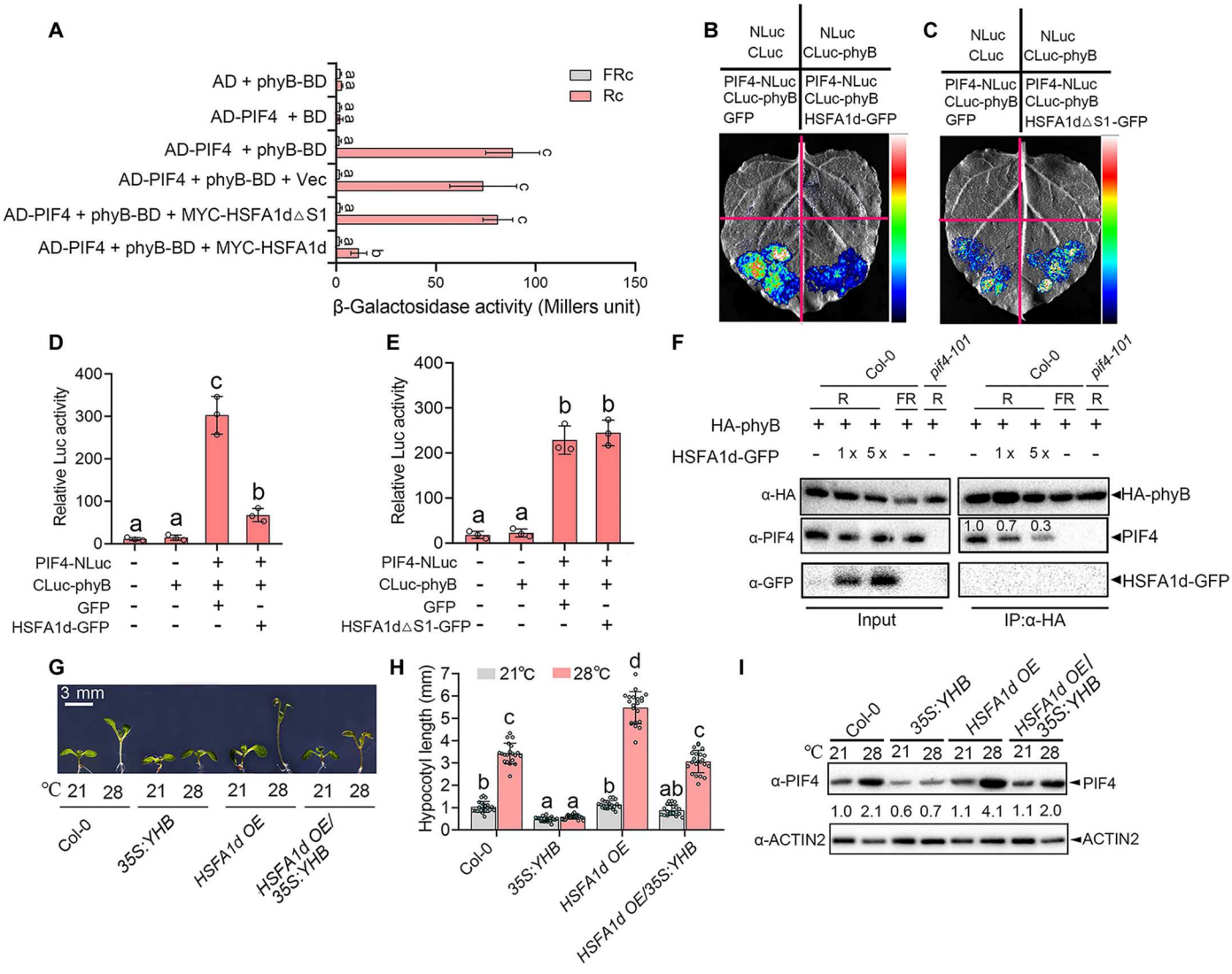

Fig. 5. HSFA1d counteracts the inhibition of phyB on PIF4 function. (**A**) Yeast three-hybrid assays showing HSFA1d inhibits the interaction of the PIF4 and Pfr form of phyB in yeast cells. Bait construct phyB-BD, prey construct AD-PIF4, and HSFA1d or HSFA1d ΔS1 (pR423-JL vector) were cotransformed into Y190 yeast cells and transformants were screened on the selective medium SD/−Leu/−Trp/−His as indicated. (**B** and **C**) LCI assays showing HSFA1d inhibits the interaction between PIF4 and phyB in vivo. The leaves of *N. benthamiana* were cotransformed with the constructs as indicated in the top panel and thereafter these plants were grown at 28°C for 24 hours. (**D** and **E**) The relative luciferase activity shown in (B) and (C). (**F**) CoIP assays showing the interaction of PIF4 and phyB in plant cells. The HA-phyB and various concentrations of HSFA1d-GFP were cotransformed into Col-0 or *pif4101* protoplasts. Then, the protoplasts were exposed to red light or far red light for 30 min at 28°C, and then the total proteins were extracted. The total proteins were incubated with anti-HA agarose beads, HA-phyB was probed by anti-HA antibody, HSFA1d-GFP was probed by anti-GFP antibody, and the coimmunoprecipitated PIF4 was detected by anti-PIF4 antibody. (**G** and **H**) Hypocotyl lengths of different genotype seedlings. Seedlings were grown in LDs at 21° or 28°C for 5 days, and then the hypocotyl lengths were detected at ZT 8 hours. (**I**) Immunoblot analysis of PIF4 protein levels in different genotype seedlings. Total proteins were extracted at ZT 8 hours from the seedlings grown at either 21° or 28°C under LDs for 5 days. Error bars represent the S.D. from three biological replicates in (A), (D), and (E) and S.D. ($n = 20$) in (H). Different letters indicate statistically significant differences (two-way ANOVA followed by a Tukey's HSD test, $P < 0.05$).

COP1 facilitates warm temperature–triggered HSFA1d nuclear localization via suppression of BIN2-directed HSFA1d phosphorylation

Then, we determined how warm temperature triggers the nuclear localization of HSFA1s in the light. A recent study reported that BIN2, known as a key regulator of BR signaling and photomorphogenesis, could phosphorylate HSFA1d and inhibit its nuclear localization (*46*). In addition, COP1, another central regulator of daytime thermomorphogenesis, was shown to inhibit BIN2 activity to promote the skotomorphogenesis (*32*). We hypothesize that there may be a functional link between HSFA1d and COP1-BIN2 module. To test this, we overexpressed HSFA1d-GFP in the *bin2-1* (gain-of-function mutant of BIN2) and *cop1-5* (COP1 knockout mutant) background, respectively (fig. S11, A and B). As expected, we found that hypocotyl elongation at high temperature was impaired in the *cop1-5* and *bin2-1* mutants, and ectopic expression of HSFA1d could not rescue the thermomorphogenesis defects of these two mutants, indicating that either the inactivation of COP1

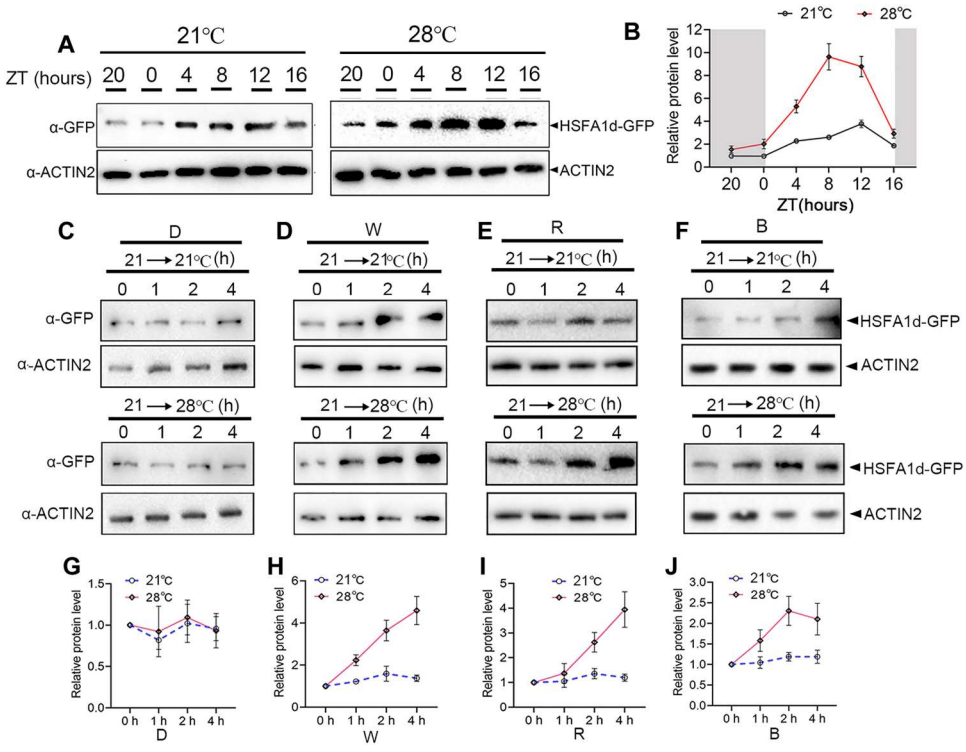

Fig. 6. Warm temperature promotes HSFA1d protein accumulation in a light-dependent manner. (**A**) Diurnal accumulation levels of HSFA1d-GFP proteins. Seedlings were grown in LDs at either 21° or 28°C for 5 days. Samples were collected every 4 hours during a cycle of 24 hours. HSFA1d-GFP proteins were analyzed using immunoblot by anti-GFP antibody and ACTIN2 was used as a loading control. (**B**) Quantification of HSFA1d-GFP proteins in the Western blots shown in (A). The intensities of detected bands were quantified from three independent experiments using ImageJ. Protein levels were normalized to ACTIN2 and expressed relative to levels of 21°C-grown *35S:HSFA1d-GFP* seedlings at ZT0. Error bars represent S.D. ($n = 3$). (**C** to **F**) Immunoblot assays showing the levels of HSFA1d-GFP proteins after exposure to 28°C under dark (D), white light (W), red light (R), and blue light (B). *35S:HSFA1d-GFP* seedlings were grown in continuous D, W, R, and B for 5 days at 21°C and then transferred to 28°C at ZT0 under the same light conditions for the indicated time periods. HSFA1d-GFP proteins were analyzed using immunoblot by anti-GFP antibody and ACTIN2 was used as a loading control. (**G** to **J**) Quantification of HSFA1d-GFP proteins in Western blots shown in (C) to (F). The intensities of detected bands were quantified from three independent experiments using ImageJ. Protein levels were normalized to ACTIN2 and expressed relative to levels at 0 hours.

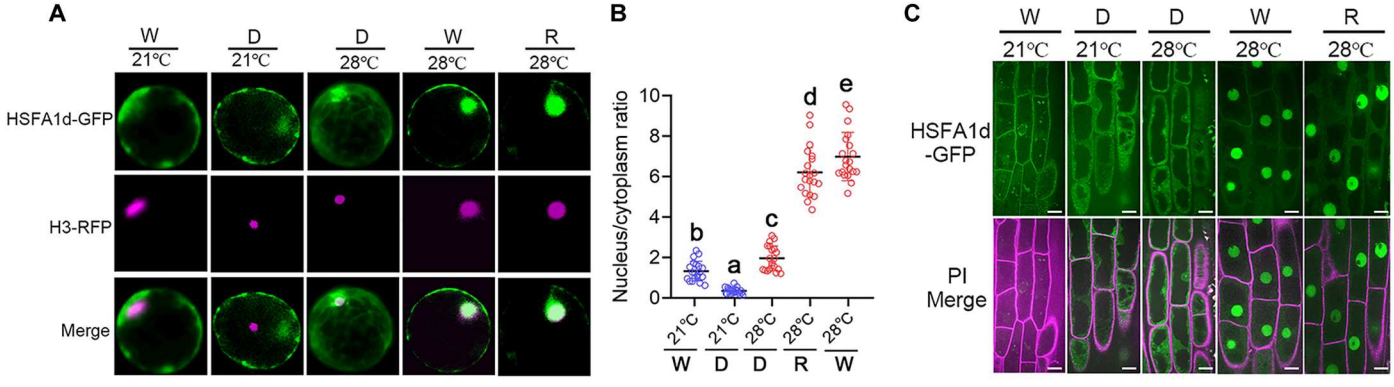

Fig. 7. Warm temperature promotes nuclear localization of HSFA1d in the light. (**A** and **B**) Nuclear and cytoplasmic fluorescence signals of HSFA1d-GFP in *Arabidopsis* mesophyll protoplast cells. Protoplast cells that expressed HSFA1d-GFP were exposed to different combinations of temperature and light conditions for 3 hours and then GFP fluorescence signals were detected. Boxplots (B) show the ratio of nuclear to cytoplasmic signals of HSFA1d-GFP. Nuclear and cytoplasmic fluorescence signals of HSFA1d-GFP from more than 20 protoplasts were measured using ImageJ. Error bars represent S.D. ($n = 20$) and different letters indicate significant differences (one-way ANOVA followed by a Tukey's HSD test, $P < 0.05$). (**C**) Nuclear and cytoplasmic fluorescence signals of HSFA1d-GFP in the root tips of *35S:HSFA1d-GFP* seedlings. Seedlings were grown in continuous D, W, R, and B for 5 days at 21°C and then transferred to 28°C with the same light conditions for 3 hours and then GFP fluorescence was detected. Scale bars, 25 μm.

or the activation of BIN2 can abolish HSFA1d function in promoting thermomorphogenic hypocotyl growth (Fig. 8, A and B). When overexpressing both HSFA1d and COP1 in the *bin2-1* background, the defect of *bin2-1* in thermomorphogenetic growth was largely rescued, suggesting that COP1 can offset the inhibitory effect of BIN2 on HSFA1d (Fig. 8, A and B). Consistent with thermomorphogenic growth phenotypes of these mutants, warm temperature–induced accumulation of PIF4 proteins was greatly enhanced in *HSFA1d OE*/Col-0 plants, but totally abolished in *bin2-1* and *cop1-5* background, while PIF4 protein accumulated to a similar level in Col-0 and *HSFA1d OE/COP1 OE/bin2-1* seedlings at 28°C, suggesting that COP1 could counteract the inhibition of BIN2 on HSFA1d-promoted PIF4 accumulation at 28°C (fig. S11C).

COP1, as an E3 ubiquitin ligase, often affects its substrate stability. We then explored whether COP1 affects the protein abundance of HSFA1d at either 21° or 28°C under different light conditions. As shown in fig. S11D, there was no difference in the abundances of HSFA1d proteins in Col-0 and *cop1-5* in both dark and light conditions, and knockout of COP1 could not affect the warm-induced HSFA1d accumulation in either white or red light, indicating that COP1 is not involved in regulating HSFA1d stability in different light conditions under normal or warm temperatures. We then analyzed the subcellular localization of HSFA1d in these backgrounds at 21° and 28°C in the light. Notably, HSFA1d failed to translocate from cytoplasm into the nuclear in both *cop1-5* and *bin2-1* mutant at 28°C in the light (Fig. 8C). However, jointly overexpressing HSFA1d and COP1 in *bin2-1* could effectively restore the high temperature–triggered nuclear localization of HSFA1d in *bin2-1* mutant (Fig. 8C). Consistently, transient transformation assays in tobacco leaves showed that COP1 and BIN2 produce opposing effects on HSFA1d at 28°C under light—the first promoting but the second inhibiting HSFA1d nuclear localization—and that

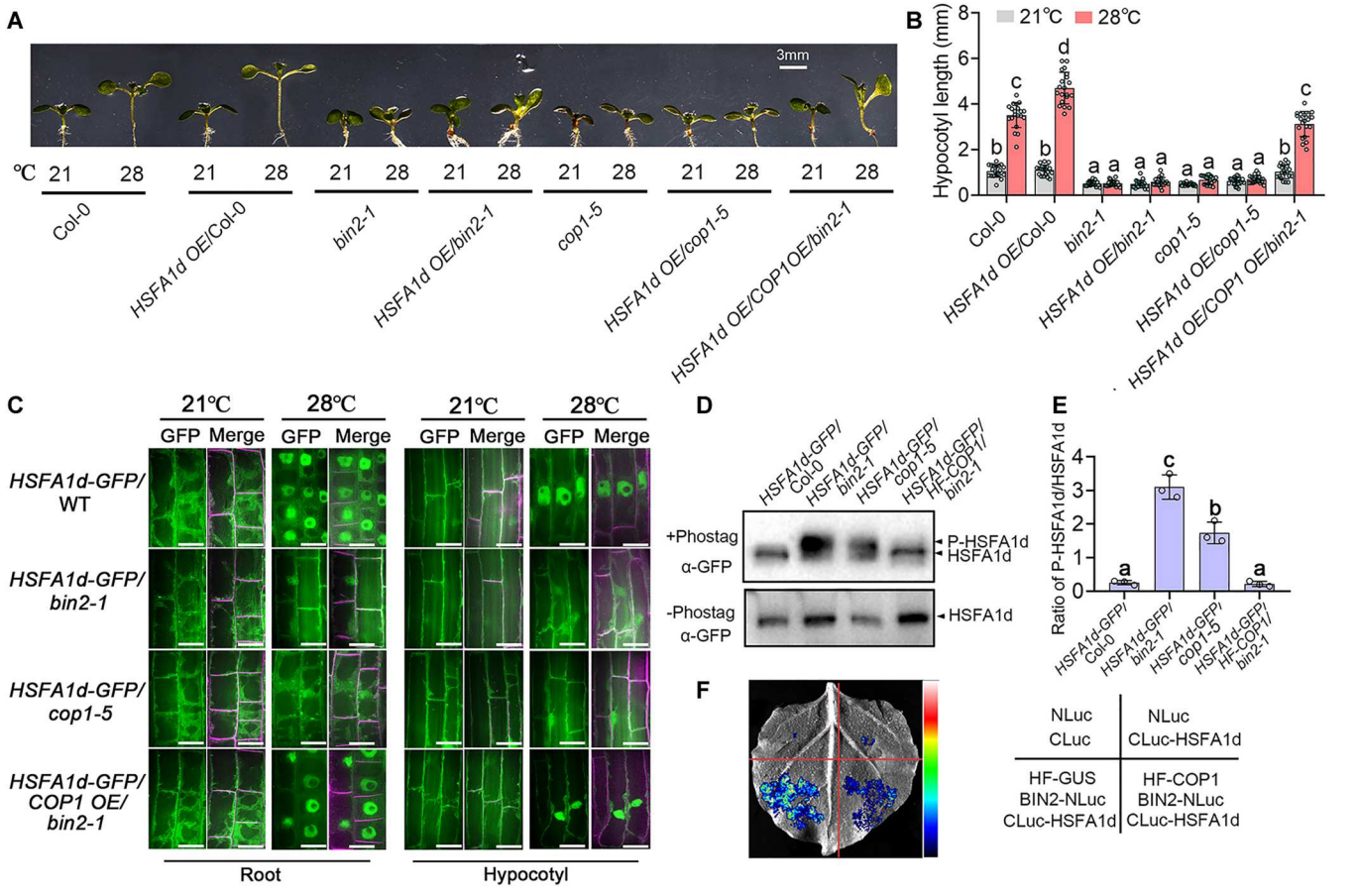

Fig. 8. COP1 inhibits BIN2-mediated inactivation of HSFA1d. (**A** and **B**) Hypocotyl lengths of indicated genotype seedlings. Seedlings were grown in LDs at either 21° or 28°C for 5 days, and then the hypocotyl lengths were measured at ZT8. Error bars represent S.D. (n = 20). Different letters indicate statistically significant differences (two-way ANOVA followed by a Tukey's HSD test, $P < 0.05$). (**C**) Nuclear and cytoplasmic fluorescence signals of HSFA1d-GFP in the roots (left) and hypocotyl (right) of indicated genotype seedlings. Seedlings were grown in continuous white light conditions for 5 days at 21°C and then transferred to 28°C with the same light conditions for 3 hours and then the GFP fluorescence was detected. Plasma membrane was labeled with PI. Scale bars, 25 μm. (**D**) In vivo phosphorylation of HSFA1d by BIN2 in a Phos-tag mobility shift assay. The *HSFA1d-GFP/Col-0*, *HSFA1d-GFP/bin2-1*, *HSFA1d-GFP/cop1-2*, and *HSFA1d-GFP/HF-COP1/bin2-1* transgenic seedlings were grown in continuous white light for 5 days at 21°C and then transferred to 28°C with the same light conditions for 3 hours and the HSFA1d-GFP proteins were collected with anti-GFP beads. The samples were resolved in phos-tag or regular gel and detected with anti-GFP antibody. (**E**) The ratio of phosphorylated HSFA1d to dephosphorylated HSFA1d in (D). Band intensity was determined from three independent experiments using ImageJ. P-HSFA1d represents phosphorylated HSFA1d. Error bars indicate S.D. (n = 3) and different letters denote statistical differences ($P < 0.05$, two-way ANOVA followed by a Tukey's HSD test). (**F**) LCI assays showing COP1 inhibits the interaction between HSFA1d and BIN2 in vivo. Leaf epidermal cells of *N. benthamiana* were cotransformed with the constructs as indicated. A sample representative image is shown.

COP1 can counteract the BIN2-directed inhibition of HSFA1d nuclear translocation (fig. S11, E and F). In addition, we detected the effects of Bikinin, an inhibitor of GSK3 kinase on the cellular localization of HSFA1d-GFP in *HSFA1d OE/bin2-1* plants at either 21° or 28°C. As shown in fig. S12A, Bikinin treatment leads to enrichment of HSFA1d in the nucleus under 21°C in *HSFA1d-GFP/bin2-1* plants, and this enrichment was further enhanced by warm temperature, suggesting that inhibition of BIN2 activity can recover the nuclear localization of HSFA1d-GFP in *HSFA1d-GFP/bin2-1*. Together, these results suggest that COP1 mediates high temperature–induced nuclear localization of HSFA1d and suppresses the inhibitory effect of BIN2 on HSFA1d.

We further explored the influences of warm temperature on BIN2 activity. The phosphorylation status of BES1, a well-known substrate of BIN2 that can reflect its endogenous activity (*61*), was examined in Col-0 seedlings under different ZT times at either 21° or 28°C. As shown in fig. S12 (B and C), the proportion of phosphorylated BES1 markedly increased in the daytime and decreased at night in Col-0 seedlings grown under 21°C, while a high proportion of unphosphorylated BES1 was present both during the daytime and at night in the plants grown under warm conditions. Consistently, the phospho-Tyr^{200} of BIN2, which can reflect its kinase activity (*61*, *62*), was also detected using an anti-pTyr antibody. We observed that notable levels of the phospho-Tyr^{200} of BIN2 were detected during the daytime and dropped after dusk at 21°C, while the phospho-Tyr^{200} of BIN2 was almost undetectable in both day and night under 28°C (fig. S12, D and E). These results indicated that BIN2 kinase activity is activated during the daytime under normal temperature, while warm temperature can inhibit BIN2 activity in both day and night. Then, we examined HSFA1d phosphorylation at both ZT 0 and ZT 8 in *HSFA1d-GFP*/Col-0 seedlings, grown under either 21° or 28°C using a phostag gel. As shown in fig. S12 (F and G), phosphorylated HSFA1d notably accumulated at ZT 8 under 21°C, but did not under 28°C, indicating that warm temperature impaired the HSFA1d phosphorylation, evidencing that BIN2-mediated HSFA1d phosphorylation occurs at 21°C during the day, when BIN2 activity is relatively high, whereas warm temperature inhibits BIN2 activity and so impedes HSFA1d phosphorylation.

Because BIN2 inhibits nuclear translocation of HSFA1d by phosphorylating its NLS (*46*), we subsequently performed phostag mobility shift assays to detect the phosphorylation levels of HSFA1d in different backgrounds. We found that the amount of phosphorylated HSFA1d protein (slow-migrating form) notably increased in both *bin2-1* and *cop1-5* backgrounds, as compared with that in Col-0, whereas the phosphorylated HSFA1d was almost undetectable in the *HSFA1d-GFP/HF-COP1/bin2-1* transgenic plants, indicating that COP1 suppresses the BIN2-medated HSFA1d phosphorylation (Fig. 8, D and E). Then, we tested whether COP1 inhibits the interaction between BIN2 and HSFA1d, as COP1 was previously reported to interfere with the interaction between BIN2 and PIF3 (*63*). Our LCI and BiFC assays in tobacco leaves revealed that the interaction between BIN2 and HSFA1d in the nucleus was greatly reduced when COP1, but not the HF-GUS, was coexpressed in tobacco leaves (Fig. 8F and fig. S13). Altogether, these results support that COP1 facilitates the warm temperature–triggered HSFA1d nuclear localization by suppressing the BIN2-mediated HSFA1d phosphorylation.

HSFA1 factors are required for thermo-acclimation

Previous studies have shown that high ambient temperature can enhance the leaf cooling capacity via various thermomorphogenic responses, including elongated architecture, hyponastic growth, and thinner leaves, consequently improving plant acclimation and survival to extremely high temperatures (*10*, *64*, *65*). We further tested whether HSFA1 factors are required for plants′ adaptive survival of HS. As previous studies reported, wild-type seedlings grown at 28°C exhibited a significantly increased tolerance to 45°C HS as compared with those grown at 21°C, while such adaptive thermotolerance was abolished in the mutant *eTK* (fig. S14, A and B). Additionally, HSFA1d-overexpressing plants showed significantly higher HS tolerance than the wild type at both 21° and 28°C, indicating that HSFA1d can promote both basal and adaptive thermotolerance (fig. S14, A and C). To investigate whether warm temperature affects HSFA1-targeted genes expression, we examined the patterns of diurnal expression in *HSFA2*, a well-characterized target gene of HSFA1 factors, in wild-type, *eTK* and *HSFA1d OE* plants grown at 21° and 28°C. When compared to the plants grown at 21°C in LDs, warm condition–grown plants had increased expression of *HSFA2* during the day, but such induction was impaired in *eTK* (fig. S14D). Furthermore, the expression of *HSFA2* in *HSFA1d*-overexpressing plants was significantly increased at both 21° and 28°C during the daytime, compared to that in wild type (fig. S14E). The results here provided support that higher growth temperature can effectively promote plant thermotolerance and *HSFA2* expression during the day, and that this process is dependent on HSFA1 factors.

DISCUSSION

During summers, plants often experience high ambient temperatures during the daytime, and they need to simultaneously sense and respond to both light and high-temperature signals, two cues with contrasting effects on thermo-adaptive growth. To survive, plants must coordinate these two environmental cues, but the underlying mechanisms are not fully understood.

Here, we found strong evidence that the heat shock response regulators, HSFA1s, promote daytime thermomorphogenic adaptive growth by inhibiting the phyB signaling–mediated PIF4 degradation during the warm LDs (Fig. 9). At the night, the temperature is relatively lower than in the daytime: The levels of HSFA1s are low and preferentially located in the cytoplasm of *Arabidopsis* cells, which results in the inactivation of HSFA1s and causes the failure to promote the thermomorphogenic hypocotyl growth (Fig. 9). During the warm daytime, plants require a moderate amount of active phyB Pfr form to trigger light responses on the one hand, and PIF4 needs to be stabilized to avoid the degradation induced by these active phyB on the other hand, enabling plants to acclimate to the high temperature. Therefore, HSFA1s accumulated and translocated into the nucleus from cytoplasm, where HSFA1s interacts with PIF4 and inhibits the interaction between PIF4 and active phyB Pfr. This further allows PIF4 accumulation to trigger the thermoresponsive genes, such as *YUC8* expression, and consequently promote daytime thermomorphogenesis (Fig. 9). Additionally, under the daytime warm conditions, a major daytime thermal regulator, COP1, facilitates the nuclear localization of HSFA1d by inhibiting BIN2-directed HSFA1d phosphorylation (Fig. 9). More specifically, daytime warm temperature–activated HSFA1s are

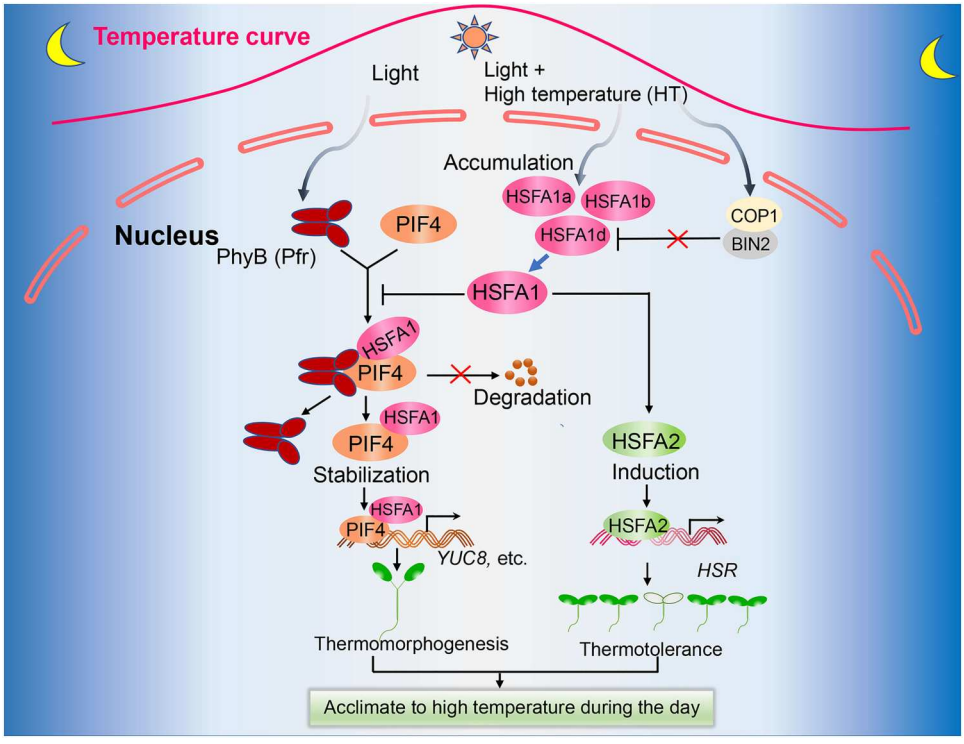

Fig. 9. Model for HSFA1-mediated daytime thermomorphogenic acclimation. Plants grown in the field often experience warm summer temperatures that overlap with enhanced light input. In such conditions, COP1 inhibits the interaction between HSFA1d with BIN2 on the one hand, allowing HSFA1d to move into the nucleus; on the other hand, warm temperatures can promote HSFA1s protein accumulation in a light-dependent manner. In the nucleus, HSFA1s and PIF4 form a stable complex and provide continuous protection of PIF4 from the light-activated form of phyB, thus protecting and stabilizing PIF4 in the light, which facilitates thermomorphogenic hypocotyl adaptation growth under daytime warm conditions. In addition, the warm temperature induces *HSFA2* expression during the daytime via HSFA1 regulators, which triggers heat shock responses and confers thermotolerance.

required for thermo-acclimation and survival of HSs occurring around the middle of the day. Warm temperature can induce *HSFA2*, a critical gene required for thermotolerance, with the expression peaking at the middle of the day, this process being dependent on HSFA1s (Fig. 9). Our presented genetic and molecular evidence strongly suggests that HSFA1 factors act as a key node that coordinates phyB-mediated light responses and PIF4-controlled thermal acclimation growth during the warm daytime.

Functioning as the central hub of light and temperature signaling pathways, PIF4 is regulated at multiple levels in sophisticated manners by both light and temperature signals. At the transcriptional level, multiple transcriptional factors, such as CCA1/LHY (*66*), BZR1 (*54*), TCP proteins (*52*), and ELF3-ELF4-LUX–constituted evening complex (*25*, *30*), directly bind to the promoter of PIF4 thereby modulating the high temperature–triggered expression of PIF4. In addition, several types of regulators, including ELF3, BZR1, HFR1, TOC1, CRY1, and UVR8, can control the transcriptional activity of PIF4 via the interaction with PIF4 (*50*, *54*, *55*, *65*, *67*, *68*). At the posttranslational level, phyB-mediated degradation is considered to function as a central pathway that controls PIF4 protein stability (*34*, *69*, *70*). PhyB appears to trigger the phosphorylation and degradation of PIF4 during the daytime, as a large amount of PIF4 proteins are accumulated in *phyB* mutant in the light (*33*); however, PIF4 under warm temperatures can accumulate to reach high levels under the continuous light. This implies that warm-temperature signals can be antagonistic to the degradation of PIF4 induced by light-activated phyB signaling, in which warm-triggered regulators maintain the stability of PIF4 under light conditions (*33*, *71*). Unlike these regulators controlling the transcripts and activity of PIF4, our results showed that HSFA1s specifically function to prevent PIF4 from combining to active Pfr phyB under simultaneous light and temperature conditions, thus stabilizing PIF4 protein during the daytime (Figs. 4, D to G, and 5 and fig. S7C). A similar regulatory mode is mediated by CBF1, an AP2/ERF-family transcription factor essential for plant cold acclimation, to promote hypocotyl elongation under low ambient temperatures by facilitating PIF4 and PIF5 accumulation in the light (*60*). It seems likely that different temperature stress regulators may be utilized to regulate growth responses by distinct temperature ranges via modulating the phyB-PIFs module, which allows for the integration of light and various temperature signals.

We observed that HSFA1s particularly promote thermomorphogenic hypocotyl elongation during the daytime, but do not affect the thermal response of hypocotyl at nighttime. The rhythmic levels of the transcripts of *HSFA1s* have been reported to show higher levels during the day, resulting in a stronger thermotolerance of plants during the daylight period (*72*). In response to warm temperatures, *HSFA1d* gene shows a similar expression pattern to what was observed in the previous study, peaking at the middle of the day and then reducing after dusk under LD conditions. Accordingly, the abundance of HSFA1d proteins is increased during the day in response to the elevated temperature, and this process is dependent

on light regimes. A previous study found that phyB-mediated light signals prime the APX2-mediated detoxification reaction of reactive oxygen species, a well-known biochemical process that mediates the acquisition of thermotolerance under high-temperature conditions; meanwhile, light signaling influences the HSFA1-stimulated activation of *APX2* transcription, which is otherwise responsive primarily to stressful high temperatures (*73*). Therefore, it seems likely that light signaling triggers HSFA1s′ functions under both warm temperature and stressful temperature. It is interesting to investigate the direct link between the photoreceptor and HSFA1s at the elevated temperature during the day, which may form a positive feedback regulation pathway to ensure PIF4 stabilization under the warm daytime, enabling plants to get the adaptive thermo-responses to maximize survival of HS.

HSFA1 factors were previously identified as master regulators in heat shock response (*39*, *40*). In addition to their roles in stress responses, HSFA1s appear to regulate adaptive growth in response to environmental cues. The *hsfa1a/1b/1d/1e* quadruple mutants (*QK*) had a defect in rosette growth and very small size at normal temperature, and more severe growth retardation was observed in the triple mutants relative to that in WT after recovery from freezing stress, implying that HSFA1s are likely required for plant growth under stress (*39*, *44*). Our results showed that HSFA1s appear to play positive roles in promoting hypocotyl growth under warm temperature (Fig. 2). Both warm temperature and stress temperatures activate HSFA1 factors, which act upon both warm-induced growth and stress responses; thus, there emerges a quite straightforward research question: How are these dual functions realized? We argue that HSFA1 factors may combine with different regulators to mediate different temperature responses. Under cold conditions, HSFA1s can interact with NONEXPRESSOR OF PR1, the main regulator of plant immunity responses, to promote the induction of HSFA1-regulated genes and cold tolerance (*44*). In response to extreme high temperature, HSFA1s heterodimerize with BES1 facilitating their activity in HSE binding, thus triggering HS responses (*47*). Our results reveal that HSFA1 can activate several PIF4 target genes, which are involved in auxin signaling and cell wall and light response pathways, via stabilization of PIF4 protein under daytime warm temperature (Figs. 3 and 4). Future studies should focus on the precise mechanisms that regulate the combination and dissociation of HSFA1 with its interactors in response to fluctuating temperature cues.

As already mentioned, the nuclear localization of HSFA1s enables their key function in triggering the expression of HSF-regulated genes (*40*, *74*). For instance, under normal conditions, HSFA1d is prominently localized in the cytosol, while HSFA1d moves into the nucleus upon heat shock or light excess (*40*, *74*). The data obtained in this study support the idea that nonstress high temperature triggers translocation of HSFA1s from the cytoplasm into the nucleus in a light-dependent pathway. The nuclear localization of HSFA1d is currently thought to be controlled by two pathways: One pathway is mediated by HSP70/HSP90 proteins that promote cytoplasmic retention of HSFA1d via binding to its temperature-dependent repression (TDR) domain under normal temperatures (*72*); the other is mediated by BIN2-directed phosphorylation of the NLS motif of HSFA1d which resulted in a constant cytoplasm localization of HSFA1d (*46*). Upon warm temperature, the activity of BIN2 is markedly reduced by an unknown mechanism, which may lead to a reduction of phosphorylation level of HSFA1d, allowing HSFA1d to retain in the nucleus. In addition, COP1, another integrator of light and temperature signals, can prevent the combination of BIN2 with HSFA1d in the nucleus, which then remove the inhibition of BIN2 on HSFA1d nuclear localization. A similar regulatory pattern was reported previously in which COP1 interferes with the interaction between BIN2 and PIF3 to stabilize PIF3 (*63*). Warm temperature can trigger the nuclear import of COP1 under both the light and dark conditions, thus enabling COP1 to continuously transport warm temperature signals into thermal responses (*31*, *75*). However, although darkness constantly induces COP1 nuclear localization and BIN2 activity is low in the dark (*62*, *76*), we did not observe nuclear translocation of HSFA1d even under elevated temperature in the dark (Fig. 7C). One plausible explanation is that HSFA1d proteins may be constrained in the cytoplasm in the dark by HSP70/HSP90 (*74*). Two other interesting issues that need to be investigated are (i) whether HSP70/HSP90 are involved in the regulation of HSFA1d-mediated thermomorphogenesis and (ii) how daytime warm temperature derepresses the HSP70/HSP90-directed inhibition of HSFA1d.

In conclusion, our study demonstrates that the regulators of heat response, HSFA1s, represent an integration node for light and warm temperature signaling, which coordinates thermomorphogenic acclimation responses via modulating phyB-PIF4 module, thus allowing plants to better respond and adapt to the daytime high temperature. To sum up, our study unveils a regulatory pathway for daytime thermomorphogenic acclimation growth mediated by HSFA1s and PIF4 factors.

MATERIALS AND METHODS

Plant materials and construction of transgenic plants

All the mutants or transgenic plants used in this study were in the *Arabidopsis* Columbia (Col-0) background, unless indicated otherwise. The *pif4101* (*57*), *phyB*-9 (CS6217), the BIN2 gain-of-function mutant *bin2-1* (*77*), *cop1-5* (CS6259), and the *35S:PIF4-MYC* (*PIF4OX*) (*54*) have all been previously described in detail. The T-DNA insertion mutants *hsfa1d-1* (SALK_022404) and *hsfa1d-2* (SALK_018552) were obtained from the Arabidopsis Stock Centre. The triple mutants of HSFA1s, including *hsfa1b/1d/1e* (*aTK*), *hsfa1a/1d/1e* (*bTK*), *hsfa1a/1b/1e* (*dTK*), and *hsfa1a/1b/1d* (*eTK*) (*39*), were supplied by Y.-Y. Charng. The *eTK/pif4101* and *PIF4OX/eTK* multiple mutants were generated by genetic crosses.

To generate *pHSFA1d:HF-HSFA1d/Col-0*, *pHSFA1a:HF-HSFA1a/eTK, pHSFA1b:HF-HSFA1b/eTK, pHSFA1d:HF-HSFA1d/eTK*, and *pHSFA1e:HF-HSFA1e/eTK*, about 2000-bp promoter fragments from HSFA1a, HSFA1b, HSFA1d, and finally HSFA1e were cloned from *Arabidopsis* genomic DNA, then used to replace the CaMV 35S promoter in the pCM1307-FLAG-HA binary vector, respectively (*78*), and then the full-length coding sequences were fused to the recombinant plasmids, and the expression constructs were transformed into Col-0 or *eTK* background by the floral dip method. The *35S:YHB*-overexpressing plants were generated as before with minor modification (*79*). $PHYB^{Y276H}$ mutant cDNA were generated by overlapping extension PCR using the primers listed in table S1. The mutagenized cDNA was excised with Sal I and Spe I restriction enzymes and cloned into the similarly restricted pCAMBIA1307-FLAG-HA vector. Then, the expression construct was transformed into Col-0 background and

overexpressed, driven by the Cauliflower Mosaic Virus (*CaMV*) *35S* promoter.

To generate *35S:HSFA1d-GFP/Col-0* (*HSFA1d OE*), *35S:HSFA1d-GFP/pif401* (*HSFA1d OE/pif4-101*), *35S:HSFA1d-GFP/35S:YHB* (*HSFA1d OE/ 35S:YHB*), *35S:HSFA1d-GFP/cop1-5* (*HSFA1d OE/cop1-5*), and *35S:HSFA1d-GFP/bin2-1*(*HSFA1d OE/bin2-1*), the full-size HSFA1d-coding cDNA was cloned to PCAMBIA-1300-eGFP vector and was overexpressed driven by the CaMV 35S promoter in the indicated background.

Plant growth conditions and treatments

The seeds of all plants involved in experiments were sterilized with 70% (v/v) ethanol and 0.1% Triton X-100 and planted on Murashige & Skoog (1/2 MS) medium. They were vernalized at 4°C for 3 days in the dark and then allowed to germinate under LDs (LDs, 16-hour light/8-hour dark photoperiod) or short conditions (SDs, 8-hour light/16-hour dark photoperiod) using white light illumination (120 μmol m^{-2} s^{-1}) inside the growth chamber at 21°C. In the thermomorphogeneic growth response assays, seedlings were grown at either 21° or 28°C under LDs for another 5 days, and then the temperature-treated seedlings were photocopied. Thereafter, the hypocotyl lengths were measured with NIH ImageJ software (http://rsb.info.nih.gov/nih-image/), using 15 to 20 seedlings being measured per genotype and condition.

RNA isolation and gene expression analysis

For the gene expression analysis, 5-day-old seedlings grown at 21°C under LD conditions were transferred into 28°C at ZT0 under LD, and the whole seedlings were harvested at ZT8 for RNA extraction. Extraction of total RNA from plant tissues followed previous protocols (*80*). Briefly, an RNeasy Mini Kit (Qiagen) was used to extract the total RNA from 50 mg of seedlings. The RNA was reverse-transcribed into cDNA using the M-MLV Reverse Transcriptase Kit (Invitrogen) following the manufacturer′s instructions. Gene transcript levels were determined by reverse transcription–mediated quantitative PCR (RT-qPCR) on the CFX96 TM RealTime System (Bio-Rad) using 2 × perfect Start Green qPCR SuperMix (Transgene) as previously described (*80*). *ACITN2* was used as the internal control. All primers used for qRT-PCR are listed in table S1. Difference fold in gene expressions was calculated using the $2^{-\Delta\Delta Ct}$ method and three biologic replicates were conducted.

For the transcriptome analyses, the Col-0 and *eTK* seedlings were grown at 21°C under LD conditions for 5 days, and then transferred into 28°C at ZT0 under LD. The samples were harvested at ZT8 and total RNA was extracted using the same procedure as qRT-PCR. Sequencing was performed on the NovaSeq 6000 platform of Biomarker Technologies. Mapping of the sequence reads to the *Arabidopsis* genome was analyzed by STAR software. Feature Counts with default parameters was used to calculate the gene read counts, and DESeq2 was used to analyze differential gene expression. We defined differentially expressed genes as those followed by a twofold expression difference with $P < 0.05$. For the GO analysis, the significance testing was performed using the hypergeometric distribution, and the resulting *P*-values were subjected to multiple testing correction using the Benjamini-Hochberg method, which was implemented using the R package "ClusterProfiler" (*81*).

ChIP-quantitative PCR assays

ChIP-quantitative PCR assays were performed as before (*65*). Briefly, the wild-type and *pHSFA1d:HF-HSFA1d/Col-0* were grown at either 21° or 28°C under LD conditions for 5 days, and then 2 g of plants was harvested at ZT 8 and the samples were cross-linked for 30 min in 1% formaldehyde solution under vacuum. Chromatin was isolated and sonicated five times (15 s on and 15 s off) to generate DNA fragments with size ranging from 200 to 1000 base pairs (bp). The sonicated chromatin complex was immunoprecipitated by anti-HA Affinity gel (Sigma, E6779). After reverse cross-linking, the DNA fragments were precipitated with 70% ethanol at −20°C for 30 min. Then, the precipitated DNA was analyzed by a real-time PCR. Enrichment was calculated as the ratio between *pHSFA1d:HF-HSFA1d/Col-0* (grown at 21° and 28°C) and Col-0 grown at 21°C, normalized to that of *TA3*. Primers for the ChIP-qPCR are listed in table S1.

Immunoblotting

Seedlings (100 mg) grown on 1/2 MS plates for 7 days were collected and ground in liquid nitrogen. For protein extraction, the ground samples were thoroughly suspended in equal volumes of 2 × SDS loading buffer (100 mM tris-Cl, pH 6.8, 4% SDS, 20% glycerol, 0.02% bromophenol blue, and 1.4% β-mercaptoethanol) and then the suspension was heated for 12 min at 98°C. Proteins were separated on 10% SDS-PAGE and blotted on the immobilon PVDF membranes (Merck Millipore, IPVH00010) using the Bio-Rad transfer system.

The primary antibodies anti-Myc (Cwbiotech, catalog no. cw0299M), anti-GFP (Abmart), anti-PIF4 (ABclonal, catalog no. A20725), anti-β-ACTIN (Cwbiotech, catalog no. cw0264A), anti-MBP (New England Biolabs, catalog no. E8023), and anti-His (Abcam, catalog no. ab18184) were used for detected Myc-PIF4, HSFA1d-GFP, PIF4, ACTIN2, MBP-HSFA1d, and His-PIF4, respectively. The Goat anti-mouse immunoglobulin G (IgG)–horseradish peroxidase (HRP; Thermo Fisher Scientific, catalog no. 31430) was used as the secondary antibody in the immunoblot assays with anti-GFP, anti-PIF4, anti-β-ACTIN antibodies and anti-HIS, and Goat anti-rabbit IgG-HRP (Thermo Fisher Scientific, catalog no. 31460) was used as the secondary antibody in the immunoblotting assays with anti-Myc and anti-His antibodies. Chemical signals were detected via chemiluminescence using a Super signal kit (Merck Millipore). Protein bands were quantified using ImageJ, and at least three biological replicates were performed.

Transient expression assay

The transient expression assay also followed a previous study (*82*). The 2000-bp promoter of the PIF4 target gene *YUC8* was cloned into the pGreen II 0800-LUC vector to construct a reporter. *pYUC8: LUC* reporter was cotransformed with *35S:HF-PIF4* or *35S:HF-PIF4* altogether with *35S:HSFA1d-GFP* into *pif4-101* protoplasts for the transcriptional activity assay. Firefly and Renilla luciferase signals were assayed using dual luciferase assay reagents (Promega, Madison, WI, USA) and the Berthold Centro LB960 luminometer system. *CaMV* 35S-driven REN was used as an internal control. The *LUC:REN* ratio was calculated, and the relative ratio was used as the final measurement. Luciferase data were normalized to total protein content.

Yeast two-hybrid screening assay

The PIF4 coding region was cloned into the pGBKT7 vector to generate a bait vector with PIF4 attached to the GAL4 DBD. The bait construct was further cotransformed into the yeast strain Y2H Gold (Clontech) with a prey cDNA library of hypocotyls of 7-day-old Col-0 seedlings, which had been grown under combined conditions of warm temperature (28°C) and high light input (120 μmol m^{-2} s^{-1}), all of which was constructed by fusing cDNAs with the GAL4 activation domain in the pGADT7-Rec vector. The transformants were screened on the selective medium (SD/−Leu/−Trp/−His/−Ade/X-a-GAL/AbA) plus 5 mM 3-amino-1,2,4-Triazol (3-AT); the positive clones were streaked on SD/−Leu/−Trp/−His/−Ade/X-a-GAL/AbA plus 5 mM 3-amino-1,2,4-Triazol (3-AT) and further identified by sequencing. The detailed procedure conducted was referred to in the Make Your Own "Mate & Plate" Library System User Manual and Yeast Two-Hybrid System User Manual (Clontech).

In vitro pull-down assays

The pull-down assays were performed as described previously (*78*). The full-length coding region of PIF4 was cloned into pET28a (+) vector (His Tag). The full-length or truncated coding sequence (CDS) of HSFA1d were incorporated into the pETMALc-H vector (MBP tag). His-tagged PIF4 and MBP-tagged HSFA1d proteins were expressed in the *E. coli* strains BL21 (DE3) (Transgene) and then purified using Ni-NTA agarose (Invitrogen, R901) and amylose resin (NEB), respectively. Purified MBP, MBP-HSFA1d, or MBP-HSFA1d truncated constructs were incubated with equal amounts of the affinity-purified His-PIF4 bait proteins immobilized on Ni-NTA agarose beads and then the beads were washed six times with His pull-down washing buffer (20 mM tris-HCl, pH 8.0, 150 mM NaCl, and 0.1% Triton). Bound proteins were eluted by boiling in 50 μl of 2× SDS loading buffer and used in subsequent SDS-PAGE and Western blotting. His-PIF4 bait proteins were examined by anti-His antibody and the immunoprecipitated MBP-HSFA1d proteins were detected by anti-MBP antibody.

BiFC assays

Biomolecular fluorescence complementation assays were performed as described previously (*78*). The full-length coding region of *HSFA1d* was cloned into pXY103 vector carrying a N-terminal yellow fluorescent protein (YFP) tag and *PIF4* was fused with a pXY104 vector carrying a C-terminal YFP tag. The constructs were transiently transformed into *Agrobacterium* strain GV3101. *Agrobacterium* carrying HSFA1d-nYFP and PIF4-cYFP constructs were cultured overnight in LB liquid medium containing 200 μM acetosyringone, and then the bacteria were collected. The *Agrobacterium* bacteria were resuspended using infiltration medium (10 mM $MgCl_2$,10 mM MES, pH 5.7, and 200 μM acetosyringone) to an OD_{600} (optical density at 600 nm) of 1.0. The suspensions of HSFA1d-nYFP and PIF4-cYFP *Agrobacterium* bacteria were mixed in equal ratios and introduced into *N. benthamiana* leaves. Two days after agroinfiltration, *N. benthamiana* plants were exposed to 21° or 28°C for 24 hours, and then YFP signals were detected from 530 to 560 nm using a fluorescence microscope (Leica, Wetzlar, Germany). All microscopy analyses were performed on at least three replicates.

Firefly LCI assays

The LCI assays were performed as described previously (*83*). The full-length CDS of indicated proteins were cloned into the pCAMBIA-1300-nLuc or pCAMBIA-1300-cLuc vectors, respectively. These vector constructs and control vectors were transformed into *Agrobacterium* strain GV3101. The bacteria that contain nLuc or cLuc constructs were cultured overnight and then mixed in equal ratios. The bacterial mixtures were then introduced into *N. benthamiana* leaves using a needle-less syringe. After agroinfiltration, *N. benthamiana* plants were grown under LDs (16 hours light/8 hours dark) for 2 days and then exposed to 21° or 28°C under continuous light for 24 hours. Before imaging, the leaves were sprayed with 1 mM D-luciferin and then kept in the dark for 5 min. The LUC signal was detected by a low-light cooled charge-coupled device camera (Tanon 5200, Tannon) with 15 min exposure time.

Coimmunoprecipitation assays

Coimmunoprecipitation (CoIP) assays were performed as described previously with only minor modifications (*84*). Col-0 and *pHSFA1d:HA-FLAG-HSFA1d*/Col-0 transgenic seedlings were grown at 21° or 28°C in continuous light for 5 days and then harvested at ZT8 and homogenized in 2 ml of IP buffer (10 mM tris, pH 7.5, 0.5% Nonidet P-40, 2 mM EDTA, 150 mM NaCl, 1 mM phenylmethylsulfonyl fluoride, and 1% plant protease inhibitor cocktail, AMRESCO). The homogenates were centrifuged at 12,000 rpm for 20 min at 4°C. The supernatant (100 μl) was reserved as input, and the remaining part was incubated with HA agarose beads (Sigma-Aldrich) for 2 hours at 4°C. The beads were collected and washed five times with IP buffer, and the coimmunoprecipited proteins were detected with the anti-PIF4 antibody (Abclonal). Samples immunoprecipitated from Col-0 were used as negative controls. CoIP assays were performed in triplicate using three independent protein samples.

Yeast three-hybrid assays

Yeast three-hybrid assays were also performed following previous descriptions (*60*). Briefly, bait construct phyB-BD, prey construct AD-PIF4, and HSFA1d (pR423-JL vector) were cotransformed into Y190 yeast cells while transformants were screened on the selective medium SD/−Leu/−Trp/−His. The positive clones were cultivated overnight in SD/−Leu/−Trp/−His liquid medium containing 2% glucose. The cultured yeast cells were transferred to fresh SD/−Leu/−Trp/−His liquid medium supplemented with 25 μM PCB and then shook for another 6 hours in the dark. The yeast cell cultures were then exposed to far red light (FRc) or red light (Rc) for 15 min and incubated for another 2 hours. β-Galactosidase activities were measured as described previously by liquid culture assays using 2-Nitrophenyl β-D-galactopyranoside (ONPG) as the substrate in Yeast Protocols Handbook (Clontech).

Fluorescence microscopy

Confocal microscopy was performed using an LSM880 confocal microscope equipped with a 100× oil-immersion objective (numerical aperture 1.40, Zeiss). For detection of fluorescence signals from GFP and red fluorescent protein (RFP), the signals were visualized at 488 nm (YFP) and 561 nm (RFP) exciting wavelengths with GaAsP detectors. The confocal images were exported with ZEN software. To analyze HSFA1d-GFP nuclear retention regulated by warm temperature and light in the *Arabidopsis* protoplasts, the

leaves of Col-0 plants were used for protoplast preparation. The expression vectors carrying HSFA1d-GFP or nuclear marker H3-RFP were cotransformed into the protoplast. Then, the protoplasts were exposed to darkness (D), white light (W), or red light (R) at 21° or 28°C for 3 hours. For the analysis of HSFA1d-GFP subcellular localization in plants, *35S:HSFA1d-GFP* seedlings in the indicated background were grown for 5 days under constant darkness (D), white light (W), and red light (R) either at 21° or 28°C. The roots and hypocotyls of the transgenic seedlings were subjected to GFP fluorescence imaging. The cell boundaries were differentiated by counterstaining with a concentration of propidium iodide (10 μg/ml) for 1 min. For PI fluorescence detection, excitation and emission were at 570–670 nm. For the subcellular localization analysis in the epidermal leaves of *N. benthamiana*, *Agrobacterium* strain GV3101 containing indicated combinations of constructs was injected into the leaves of 7-week-old tobacco plants using a needleless syringe. Two days after agroinfiltration of *N. benthamiana* plants, these were exposed to 21° or 28°C for 24 hours, and the GFP signals were detected. The nuclear/cytoplasmic rate was measured from at least 20 cells with ImageJ.

HS treatment

Heat shock treatment assays were performed with seedlings pregrown at 21°C for 3 days and then further grown at 21° or 28°C under LDs for another 4 days, as described previously (*62*). These seedlings were immersed in a 45°C water bath for the indicated times (0 to 20 min). Survival rates were scored after 5 days of recovery at 21°C under LDs.

Statistical analysis

Statistical tests were performed in GraphPad Prism 5.0 software and SPSS software. The band intensity of immunoblotting and fluorescence intensity were measured with ImageJ. Error bars indicate mean ± S.D. and different letters in the figures indicate the result analysis of variance (ANOVA) testing followed by a Tukey's HSD test ($P < 0.05$).

Accession numbers

All *Arabidopsis* genes reported in this study can be found at TAIR (www.arabidopsis.org), which includes the following accession numbers: *HSFA1d* (AT1G32330), *PIF4* (AT2G43010), *YUCCA8* (AT4G28720), *SUAR20* (AT5G18020), *XTR6* (AT4G25810), *ST2A* (AT5G07010), *CDF5* (AT1G69570), *5PTASE11* (AT1G47510), *phyB* (AT2G18790), *HSFA1a* (AT4G17750), *HSFA1b* (AT5G12860), and *HSFA1e* (AT3G02990).

Supplementary Materials

This PDF file includes:
Figs. S1 to S14
Legends for data sets S1 to S3
Table S1
Raw data of Western blot

Other Supplementary Material for this manuscript includes the following:
Data Sets S1 to S3

REFERENCES AND NOTES

1. J. J. Casal, J. I. Qüesta, Light and temperature cues: Multitasking receptors and transcriptional integrators. *New Phytol.* **217**, 1029–1034 (2018).
2. L. Qi, Y. Shi, W. Terzaghi, S. Yang, J. Li, Integration of light and temperature signaling pathways in plants. *J. Integr. Plant Biol.* **64**, 393–411 (2022).
3. M. Quint, C. Delker, K. A. Franklin, P. A. Wigge, K. J. Halliday, M. van Zanten, Molecular and genetic control of plant thermomorphogenesis. *Nat. Plants* **2**, 15190 (2016).
4. F. Vandenbussche, J. P. Verbelen, D. Van Der Straeten, Of light and length: Regulation of hypocotyl growth in *Arabidopsis*. *Bioessays* **27**, 275–284 (2005).
5. M.-C. Cheng, P. K. Kathare, I. Paik, E. Huq, Phytochrome signaling networks. *Annu. Rev. Plant Biol.* **72**, 217–244 (2021).
6. A. A. Arsovski, A. Galstyan, J. M. Guseman, J. L. Nemhauser, Photomorphogenesis. *Arabidopsis Book* **10**, e0147 (2012).
7. J. J. Casal, S. Balasubramanian, Thermomorphogenesis. *Annu. Rev. Plant Biol.* **70**, 321–346 (2019).
8. M. Legris, C. Nieto, R. Sellaro, S. Prat, J. J. Casal, Perception and signalling of light and temperature cues in plants. *Plant J.* **90**, 683–697 (2017).
9. P. Leivar, E. Monte, Y. Oka, T. Liu, C. Carle, A. Castillon, E. Huq, P. H. Quail, Multiple phytochrome-interacting bHLH transcription factors repress premature seedling photomorphogenesis in darkness. *Curr. Biol.* **18**, 1815–1823 (2008).
10. M. A. Koini, L. Alvey, T. Allen, C. A. Tilley, N. P. Harberd, G. C. Whitelam, K. A. Franklin, High temperature-mediated adaptations in plant architecture require the bHLH transcription factor PIF4. *Curr. Biol.* **19**, 408–413 (2009).
11. P. Leivar, P. H. Quail, PIFs: Pivotal components in a cellular signaling hub. *Trends Plant Sci.* **16**, 19–28 (2011).
12. J. Sun, L. Qi, Y. Li, J. Chu, C. Li, PIF4–mediated activation of *YUCCA8* expression integrates temperature into the auxin pathway in regulating *Arabidopsis* hypocotyl growth. *PLOS Genet.* **8**, e1002594 (2012).
13. K. A. Franklin, S. H. Lee, D. Patel, S. V. Kumar, A. K. Spartz, C. Gu, S. Ye, P. Yu, G. Breen, J. D. Cohen, P. A. Wigge, W. M. Gray, Phytochrome-interacting factor 4 (PIF4) regulates auxin biosynthesis at high temperature. *Proc. Natl. Acad. Sci. U.S.A.* **108**, 20231–20235 (2011).
14. H. Zhao, Y. Bao, PIF4: Integrator of light and temperature cues in plant growth. *Plant Sci.* **313**, 111086 (2021).
15. M. Legris, C. Klose, E. S. Burgie, C. C. R. Rojas, M. Neme, A. Hiltbrunner, P. A. Wigge, E. Schäfer, R. D. Vierstra, J. J. Casal, Phytochrome B integrates light and temperature signals in *Arabidopsis*. *Science* **354**, 897–900 (2016).
16. J.-H. Jung, M. Domijan, C. Klose, S. Biswas, D. Ezer, M. Gao, A. K. Khattak, M. S. Box, V. Charoensawan, S. Cortijo, M. Kumar, A. Grant, J. C. W. Locke, E. Schäfer, K. E. Jaeger, P. A. Wigge, Phytochromes function as thermosensors in *Arabidopsis*. *Science* **354**, 886–889 (2016).
17. J. Li, G. Li, H. Wang, X. W. Deng, Phytochrome signaling mechanisms. *Arabidopsis Book* **9**, e0148 (2011).
18. G. Bae, G. Choi, Decoding of light signals by plant phytochromes and their interacting proteins. *Annu. Rev. Plant Biol.* **59**, 281–311 (2008).
19. C. Fankhauser, M. Chen, Transposing phytochrome into the nucleus. *Trends Plant Sci.* **13**, 596–601 (2008).
20. C. Klose, A. Viczián, S. Kircher, E. Schäfer, F. Nagy, Molecular mechanisms for mediating light-dependent nucleo/cytoplasmic partitioning of phytochrome photoreceptors. *New Phytol.* **206**, 965–971 (2015).
21. V. N. Pham, P. K. Kathare, E. Huq, Phytochromes and phytochrome interacting factors. *Plant Physiol.* **176**, 1025–1038 (2018).
22. C. Klose, F. Nagy, E. Schäfer, Thermal reversion of plant phytochromes. *Mol. Plant* **13**, 386–397 (2020).
23. D. Chen, M. Lyu, X. Kou, J. Li, Z. Yang, L. Gao, Y. Li, L.-M. Fan, H. Shi, S. Zhong, Integration of light and temperature sensing by liquid-liquid phase separation of phytochrome B. *Mol. Cell* **82**, 3015–3029.e6 (2022).
24. T. Yamashino, A. Matsushika, T. Fujimori, S. Sato, T. Kato, S. Tabata, T. Mizuno, A link between circadian-controlled bHLH factors and the APRR1/TOC1 quintet in *Arabidopsis thaliana*. *Plant Cell Physiol.* **44**, 619–629 (2003).
25. M. S. Box, B. E. Huang, M. Domijan, K. E. Jaeger, A. K. Khattak, S. J. Yoo, E. L. Sedivy, D. M. Jones, T. J. Hearn, A. A. Webb, A. Grant, J. C. W. Locke, P. A. Wigge, ELF3 controls thermoresponsive growth in *Arabidopsis*. *Curr. Biol.* **25**, 194–199 (2015).
26. D. A. Nusinow, A. Helfer, E. E. Hamilton, J. J. King, T. Imaizumi, T. F. Schultz, E. M. Farré, S. A. Kay, The ELF4–ELF3–LUX complex links the circadian clock to diurnal control of hypocotyl growth. *Nature* **475**, 398–402 (2011).

27. B. Thines, F. G. Harmon, Ambient temperature response establishes ELF3 as a required component of the core *Arabidopsis* circadian clock. *Proc. Natl. Acad. Sci. U.S.A.* **107**, 3257–3262 (2010).
28. J.-H. Jung, A. D. Barbosa, S. Hutin, J. R. Kumita, M. Gao, D. Derwort, C. S. Silva, X. Lai, E. Pierre, F. Geng, S.-B. Kim, S. Baek, C. Zubieta, K. E. Jaeger, P. A. Wigge, A prion-like domain in ELF3 functions as a thermosensor in *Arabidopsis*. *Nature* **585**, 256–260 (2020).
29. K. Nozue, M. F. Covington, P. D. Duek, S. Lorrain, C. Fankhauser, S. L. Harmer, J. N. Maloof, Rhythmic growth explained by coincidence between internal and external cues. *Nature* **448**, 358–361 (2007).
30. D. Ezer, J.-H. Jung, H. Lan, S. Biswas, L. Gregoire, M. S. Box, V. Charoensawan, S. Cortijo, X. Lai, D. Stöckle, C. Zubieta, K. E. Jaeger, P. A. Wigge, The evening complex coordinates environmental and endogenous signals in *Arabidopsis*. *Nat. Plants* **3**, 17087 (2017).
31. C. Nieto, P. Catalán, L. M. Luengo, M. Legris, V. López-Salmerón, J. M. Davière, J. J. Casal, S. Ares, S. Prat, COP1 dynamics integrate conflicting seasonal light and thermal cues in the control of *Arabidopsis* elongation. *Sci. Adv.* **8**, eabp8412 (2022).
32. Y. J. Park, H. J. Lee, J. H. Ha, J. Y. Kim, C. M. Park, COP1 conveys warm temperature information to hypocotyl thermomorphogenesis. *New Phytol.* **215**, 269–280 (2017).
33. Y. Qiu, M. Li, R. J.-A. Kim, C. M. Moore, M. Chen, Daytime temperature is sensed by phytochrome B in *Arabidopsis* through a transcriptional activator HEMERA. *Nat. Commun.* **10**, 140 (2019).
34. Y. Qiu, E. K. Pasoreck, C. Y. Yoo, J. He, H. Wang, A. Bajracharya, M. Li, H. D. Larsen, S. Cheung, M. Chen, RCB initiates *Arabidopsis* thermomorphogenesis by stabilizing the thermoregulator PIF4 in the daytime. *Nat. Commun.* **12**, 2042 (2021).
35. N. Andrási, A. Pettkó-Szandtner, L. Szabados, Diversity of plant heat shock factors: Regulation, interactions, and functions. *J. Exp. Bot.* **72**, 1558–1575 (2021).
36. M. Åkerfelt, R. I. Morimoto, L. Sistonen, Heat shock factors: Integrators of cell stress, development and lifespan. *Nat. Rev. Mol. Cell Biol.* **11**, 545–555 (2010).
37. K.-D. Scharf, T. Berberich, I. Ebersberger, L. Nover, The plant heat stress transcription factor (Hsf) family: Structure, function and evolution. *Biochim. Biophys. Acta* **1819**, 104–119 (2012).
38. N. Ohama, H. Sato, K. Shinozaki, K. Yamaguchi-Shinozaki, Transcriptional regulatory network of plant heat stress response. *Trends Plant Sci.* **22**, 53–65 (2017).
39. H.-C. Liu, H.-T. Liao, Y.-Y. Charng, The role of class A1 heat shock factors (HSFA1s) in response to heat and other stresses in *Arabidopsis*. *Plant Cell Environ.* **34**, 738–751 (2011).
40. T. Yoshida, N. Ohama, J. Nakajima, S. Kidokoro, J. Mizoi, K. Nakashima, K. Maruyama, J.-M. Kim, M. Seki, D. Todaka, Y. Osakabe, Y. Sakuma, F. Schöffl, K. Shinozaki, K. Yamaguchi-Shinozaki, *Arabidopsis* HsfA1 transcription factors function as the main positive regulators in heat shock-responsive gene expression. *Mol. Genet. Genomics* **286**, 321–332 (2011).
41. U. Bechtold, W. S. Albihlal, T. Lawson, M. J. Fryer, P. A. Sparrow, F. Richard, R. Persad, L. Bowden, R. Hickman, C. Martin, J. L. Beynon, V. Buchanan-Wollaston, N. R. Baker, J. I. L. Morison, F. Schöffl, S. Ott, P. M. Mullineaux, Arabidopsis *HEAT SHOCK TRANSCRIPTION FACTORA1b* overexpression enhances water productivity, resistance to drought, and infection. *J. Exp. Bot.* **64**, 3467–3481 (2013).
42. S.-H. Han, Y.-J. Park, C.-M. Park, Light priming of thermotolerance development in plants. *Plant Signal. Behav.* **14**, 1554469 (2019).
43. J. Qian, J. Chen, Y. F. Liu, L. L. Yang, W. P. Li, L. M. Zhang, Overexpression of *Arabidopsis HsfA1a* enhances diverse stress tolerance by promoting stress-induced Hsp expression. *Genet. Mol. Res.* **13**, 1233–1243 (2014).
44. E. Olate, J. M. Jiménez-Gómez, L. Holuigue, J. Salinas, NPR1 mediates a novel regulatory pathway in cold acclimation by interacting with HSFA1 factors. *Nat. Plants* **4**, 811–823 (2018).
45. H. Liu, Y. Zhang, S. Lu, H. Chen, J. Wu, X. Zhu, B. Zou, J. Hua, HsfA1d promotes hypocotyl elongation under chilling via enhancing expression of ribosomal protein genes in *Arabidopsis*. *New Phytol.* **231**, 646–660 (2021).
46. J. Luo, J. Jiang, S. Sun, X. Wang, Brassinosteroids promote thermotolerance through releasing BIN2-mediated phosphorylation and suppression of HsfA1 transcription factors in *Arabidopsis*. *Plant Commun.* **3**, 100419 (2022).
47. P. Albertos, G. Dündar, P. Schenk, S. Carrera, P. Cavelius, T. Sieberer, B. Poppenberger, Transcription factor BES1 interacts with HSFA1 to promote heat stress resistance of plants. *EMBO J.* **41**, e108664 (2022).
48. B. Y. Chung, M. Balcerowicz, M. Di Antonio, K. E. Jaeger, F. Geng, K. Franaszek, P. Marriott, I. Brierley, A. E. Firth, P. A. Wigge, An RNA thermoswitch regulates daytime growth in *Arabidopsis*. *Nat. Plants* **6**, 522–532 (2020).
49. U. V. Pedmale, S.-S. C. Huang, M. Zander, B. J. Cole, J. Hetzel, K. Ljung, P. A. B. Reis, P. Sridevi, K. Nito, J. R. Nery, J. R. Ecker, J. Chory, Cryptochromes interact directly with PIFs to control plant growth in limiting blue light. *Cell* **164** (Pt 1–2), 233–245 (2016).
50. D. Ma, X. Li, Y. Guo, J. Chu, S. Fang, C. Yan, J. P. Noel, H. Liu, Cryptochrome 1 interacts with PIF4 to regulate high temperature-mediated hypocotyl elongation in response to blue light. *Proc. Natl. Acad. Sci. U.S.A.* **113**, 224–229 (2016).
51. H.-J. Lee, J.-H. Jung, L. Cortés Llorca, S.-G. Kim, S. Lee, I. T. Baldwin, C.-M. Park, FCA mediates thermal adaptation of stem growth by attenuating auxin action in *Arabidopsis*. *Nat. Commun.* **5**, 5473 (2014).
52. X. Han, H. Yu, R. Yuan, Y. Yang, F. An, G. Qin, *Arabidopsis* transcription factor TCP5 controls plant thermomorphogenesis by positively regulating PIF4 activity. *iScience* **15**, 611–622 (2019).
53. Y. Zhou, Q. Xun, D. Zhang, M. Lv, Y. Ou, J. Li, TCP transcription factors associate with PHYTOCHROME INTERACTING FACTOR 4 and CRYPTOCHROME 1 to regulate thermomorphogenesis in *Arabidopsis thaliana*. *iScience* **15**, 600–610 (2019).
54. E. Oh, J.-Y. Zhu, Z.-Y. Wang, Interaction between BZR1 and PIF4 integrates brassinosteroid and environmental responses. *Nat. Cell Biol.* **14**, 802–809 (2012).
55. C. Nieto, V. López-Salmerón, J.-M. Davière, S. Prat, ELF3-PIF4 interaction regulates plant growth independently of the Evening Complex. *Curr. Biol.* **25**, 187–193 (2015).
56. C. Martínez, A. Espinosa-Ruíz, M. de Lucas, S. Bernardo-García, J. M. Franco-Zorrilla, S. Prat, PIF4-induced BR synthesis is critical to diurnal and thermomorphogenic growth. *EMBO J.* **37**, e99552 (2018).
57. E. Huq, P. H. Quail, PIF4, a phytochrome-interacting bHLH factor, functions as a negative regulator of phytochrome B signaling in *Arabidopsis*. *EMBO J.* **21**, 2441–2450 (2002).
58. J.-H. Kim, H.-J. Lee, J.-H. Jung, S. Lee, C.-M. Park, HOS1 facilitates the phytochrome B-mediated inhibition of PIF4 function during hypocotyl growth in *Arabidopsis*. *Mol. Plant* **10**, 274–284 (2017).
59. R. Khanna, E. Huq, E. A. Kikis, B. Al-Sady, C. Lanzatella, P. H. Quail, A novel molecular recognition motif necessary for targeting photoactivated phytochrome signaling to specific basic helix-loop-helix transcription factors. *Plant Cell* **16**, 3033–3044 (2004).
60. X. Dong, Y. Yan, B. Jiang, Y. Shi, Y. Jia, J. Cheng, Y. Shi, J. Kang, H. Li, D. Zhang, L. Qi, R. Han, S. Zhang, Y. Zhou, X. Wang, W. Terzaghi, H. Gu, D. Kang, S. Yang, J. Li, The cold response regulator CBF1 promotes *Arabidopsis* hypocotyl growth at ambient temperatures. *EMBO J.* **39**, e103630 (2020).
61. J. Li, H. Zhou, Y. Zhang, Z. Li, Y. Yang, Y. Guo, The GSK3-like kinase BIN2 is a molecular switch between the salt stress response and growth recovery in *Arabidopsis thaliana*. *Dev. Cell* **55**, 367–380.e6 (2020).
62. J. Li, W. Terzaghi, Y. Gong, C. Li, J.-J. Ling, Y. Fan, N. Qin, X. Gong, D. Zhu, X. W. Deng, Modulation of BIN2 kinase activity by HY5 controls hypocotyl elongation in the light. *Nat. Commun.* **11**, 1592 (2020).
63. J.-J. Ling, J. Li, D. Zhu, X. W. Deng, Noncanonical role of *Arabidopsis* COP1/SPA complex in repressing BIN2-mediated PIF3 phosphorylation and degradation in darkness. *Proc. Natl. Acad. Sci.* **114**, 3539–3544 (2017).
64. A. J. Crawford, D. H. McLachlan, A. M. Hetherington, K. A. Franklin, High temperature exposure increases plant cooling capacity. *Curr. Biol.* **22**, R396–R397 (2012).
65. J.-Y. Zhu, E. Oh, T. Wang, Z.-Y. Wang, TOC1–PIF4 interaction mediates the circadian gating of thermoresponsive growth in *Arabidopsis*. *Nat. Commun.* **7**, 13692 (2016).
66. Q. Sun, S. Wang, G. Xu, X. Kang, M. Zhang, M. Ni, SHB1 and CCA1 interaction desensitizes light responses and enhances thermomorphogenesis. *Nat. Commun.* **10**, 3110 (2019).
67. P. Hornitschek, S. Lorrain, V. Zoete, O. Michielin, C. Fankhauser, Inhibition of the shade avoidance response by formation of non-DNA binding bHLH heterodimers. *EMBO J.* **28**, 3893–3902 (2009).
68. S. Hayes, A. Sharma, D. P. Fraser, M. Trevisan, C. K. Cragg-Barber, E. Tavridou, C. Fankhauser, G. I. Jenkins, K. A. Franklin, UV-B perceived by the UVR8 photoreceptor inhibits plant thermomorphogenesis. *Curr. Biol.* **27**, 120–127 (2017).
69. J. Shin, K. Kim, H. Kang, I. S. Zulfugarov, G. Bae, C.-H. Lee, D. Lee, G. Choi, Phytochromes promote seedling light responses by inhibiting four negatively-acting phytochrome-interacting factors. *Proc. Natl. Acad. Sci. U.S.A.* **106**, 7660–7665 (2009).
70. S. Lorrain, T. Allen, P. D. Duek, G. C. Whitelam, C. Fankhauser, Phytochrome-mediated inhibition of shade avoidance involves degradation of growth-promoting bHLH transcription factors. *Plant J.* **53**, 312–323 (2008).
71. S. N. Gangappa, S. V. Kumar, DET1 and HY5 control PIF4-mediated thermosensory elongation growth through distinct mechanisms. *Cell Rep.* **18**, 344–351 (2017).
72. P. J. Dickinson, M. Kumar, C. Martinho, S. J. Yoo, H. Lan, G. Artavanis, V. Charoensawan, M. A. Schöttler, R. Bock, K. E. Jaeger, P. A. Wigge, Chloroplast signaling gates thermotolerance in *Arabidopsis*. *Cell Rep.* **22**, 1657–1665 (2018).
73. S.-H. Han, Y.-J. Park, C.-M. Park, Light primes the thermally induced detoxification of reactive oxygen species during development of thermotolerance in *Arabidopsis*. *Plant Cell Physiol.* **60**, 230–241 (2019).
74. N. Ohama, K. Kusakabe, J. Mizoi, H. Zhao, S. Kidokoro, S. Koizumi, F. Takahashi, T. Ishida, S. Yanagisawa, K. Shinozaki, K. Yamaguchi-Shinozaki, The transcriptional cascade in the heat stress response of *Arabidopsis* is strictly regulated at the level of transcription factor expression. *Plant Cell* **28**, 181–201 (2016).
75. Y. J. Park, H. J. Lee, J. H. Ha, J. Y. Kim, C. M. Park, COP 1 conveys warm temperature information to hypocotyl thermomorphogenesis. *New Phytol.* **215**, 269–280 (2017).

76. O. S. Lau, X. W. Deng, The photomorphogenic repressors COP1 and DET1: 20 years later. *Trends Plant Sci.* **17**, 584–593 (2012).
77. J. Li, K. H. Nam, Regulation of brassinosteroid signaling by a GSK3/SHAGGY-like kinase. *Science* **295**, 1299–1301 (2002).
78. D. Zhang, W. Tan, F. Yang, Q. Han, H. Lin, A BIN2-GLK1 signaling module integrates Brassinosteroid and light signaling to repress chloroplast development in the dark. *Dev. Cell* **56**, 310–324.e7 (2020).
79. Y. S. Su, J. C. Lagarias, Light-independent phytochrome signaling mediated by dominant GAF domain tyrosine mutants of *Arabidopsis* phytochromes in transgenic plants. *Plant Cell* **19**, 2124–2139 (2007).
80. S. Chai, J. Chen, X. Yue, C. Li, Q. Zhang, V. Resco de Dios, Y. Yao, W. Tan, Interaction of BES1 and LBD37 transcription factors modulates brassinosteroid-regulated root forging response under low nitrogen in arabidopsis. *Front. Plant Sci.* **13**, 998961 (2022).
81. T. Wu, E. Hu, S. Xu, M. Chen, P. Guo, Z. Dai, T. Feng, L. Zhou, W. Tang, L. Zhan, X. Fu, S. Liu, X. Bo, G. Yu, ClusterProfiler 4.0: A universal enrichment tool for interpreting omics data. *Innovation* **2**, 100141 (2021).
82. W. Tan, Q. Han, Y. Li, F. Yang, J. Li, P. Li, X. Xu, H. Lin, D. Zhang, A HAT1-DELLA signaling module regulates trichome initiation and leaf growth by achieving gibberellin homeostasis. *New Phytol.* **231**, 1220–1235 (2021).
83. H. Chen, Y. Zou, Y. Shang, H. Lin, Y. Wang, R. Cai, X. Tang, J. Zhou, Firefly luciferase complementation imaging assay for protein-protein interactions in plants. *Plant Physiol.* **146**, 368–376 (2008).
84. Q. Han, W. Tan, Y. Zhao, F. Yang, X. Yao, H. Lin, D. Zhang, Salicylic acid-activated BIN2 phosphorylation of TGA3 promotes *Arabidopsis* PR gene expression and disease resistance. *EMBO J.* **41**, e110682 (2022).

Acknowledgments: We thank Y.-Y. Charng for providing HSFA1-related seeds. We also thank Y. Yin for providing the anti-BES1 antibody; J. Li for providing phyB-BD, pR423-JL vectors, and Y190 yeast strain for yeast three-hybrid assays; and J. Zhou for providing the pCAMBIA-1300-nLuc and pCAMBIA-1300-cLuc vectors. **Funding:** This work was supported by the Natural Science Foundation of China (32000217, U20A20179, and 31850410483), the Natural Science Foundation of Southwest University of Science and Technology (19zx7153), and the Sichuan Natural Science Foundation (2023NSFSC1273). **Author contributions:** Conceptualization: W.T., Y.Y., and D.Z. Investigation: W.T., J.C., X.Y., S.C., and C.L. Methodology: W.L., F.Y., and Y.G. Visualization: W.T. and D.Z. Supervision: W.T. and Y.Y. Writing—original draft: W.T. and Y.Y. Writing—review and editing: V.R.d.D., L.G.R., and D.Z. **Competing interests:** The authors declare that they have no competing interests. **Data and materials availability:** All data needed to evaluate the conclusions in the paper are present in the paper and/or the Supplementary Materials. The plant materials can be provided by Y.Y. pending scientific review and a completed material transfer agreement. Requests for the materials should be submitted to Y.Y.: yinanyao@swust.edu.cn. The RNA-seq data from this study have been deposited to the Sequence Read Archive database (https://ncbi.nlm.nih.gov/sra/) and assigned the accession number PRJNA932478.

Submitted 16 February 2023
Accepted 4 October 2023
Published 3 November 2023
10.1126/sciadv.adh1738